LEVEL II

AFTERBODY DRAG

VOLUME 1 – DRAG OF CONICAL AND CIRCULAR ARC AFTERBODIES WITHOUT JET FLOW

by

Peter R. Payne
Payne, Incorporated

and

Richard M. Hartley
Robert M. Taylor

AVIATION AND SURFACE EFFECTS DEPARTMENT

DTNSRDC/ASED-80/10

May 1980

DAVID W. TAYLOR NAVAL SHIP RESEARCH AND DEVELOPMENT CENTER
BETHESDA, MARYLAND 20084

UNCLASSIFIED

SECURITY CLASSIFICATION OF THIS PAGE (When Data Entered)

REPORT DOCUMENTATION PAGE

READ INSTRUCTIONS BEFORE COMPLETING FORM

(18) (19) DTNSRDC/ASED-80/10

2. GOVT ACCESSION NO. AD-A087 514

3. RECIPIENT'S CATALOG NUMBER

(6) 4. TITLE (and Subtitle)
AFTERBODY DRAG,
VOLUME 1, DRAG OF CONICAL AND CIRCULAR ARC AFTERBODIES WITHOUT JET FLOW,

(9) 5. TYPE OF REPORT & PERIOD COVERED
Final Report,

(14) 6. PERFORMING ORG. REPORT NUMBER
A125-1-V01-21

(10) 7. AUTHOR(s)
Peter R. Payne (Payne, Incorporated)
Richard M. Hartley (DTNSRDC)
Robert M. Taylor (DTNSRDC)

(15) 8. CONTRACT OR GRANT NUMBER(s)
N00014-77-C-0039

9. PERFORMING ORGANIZATION NAME AND ADDRESS
Payne, Incorporated
Annapolis, Maryland 21401

10. PROGRAM ELEMENT, PROJECT, TASK AREA & WORK UNIT NUMBERS
(See reverse side)

11. CONTROLLING OFFICE NAME AND ADDRESS
David W. Taylor Naval Ship R&D Center
Aviation and Surface Effects Department
Bethesda, Maryland 20084

(11) 12. REPORT DATE
May 1980

13. NUMBER OF PAGES
59

14. MONITORING AGENCY NAME & ADDRESS(if different from Controlling Office)
Naval Air Systems Command
Washington, D.C. 20361
Naval Weapons Center
China Lake, California 93555

(12) 60

15. SECURITY CLASS (of this report)
UNCLASSIFIED

15a. DECLASSIFICATION/DOWNGRADING SCHEDULE

16. DISTRIBUTION STATEMENT (of this Report)

(16) W15XZ0 F32322

APPROVED FOR PUBLIC RELEASE: DISTRIBUTION UNLIMITED

17. DISTRIBUTION STATEMENT (of the abstract entered in Block 20, if different from Report)

(17) W15XZ0 0000-
WF32322203

18. SUPPLEMENTARY NOTES

19. KEY WORDS (Continue on reverse side if necessary and identify by block number)
Base Pressure
Boattail Drag
Jet Interference
Subsonic Flow
Transonic Flow

20. ABSTRACT (Continue on reverse side if necessary and identify by block number)

The results of the afterbody drag study are presented in four volumes. Volume 1: Drag of Conical and Circular Arc Afterbodies; Volume 2: Jet Interference Effects on Subsonic Boattail Drag; Volume 3: Literature Survey; and Volume 4: Data and Analysis.

Volume 1 includes a series of charts that enable the drag of conical and circular arc afterbodies without jet flow to be determined.

DD FORM 1 JAN 73 1473 EDITION OF 1 NOV 65 IS OBSOLETE
S/N 0102-LF-014-6601

UNCLASSIFIED

SECURITY CLASSIFICATION OF THIS PAGE (When Data Entered)

277 770

(Block 10)

Program Elements:
63361N
62332N
62241N

Task Area Numbers:
W15X20000
WF32.322.203
WF41.421.201

Work Unit Numbers:
1660-234
1660-235

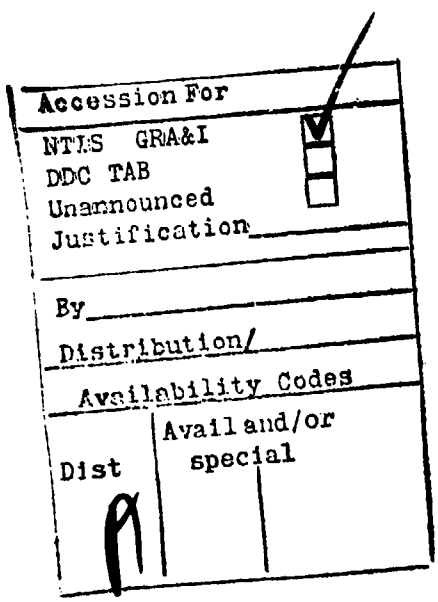

TABLE OF CONTENTS

LIST OF FIGURES

NOTATION

A	Area
A_j	Jet exit area
A_m	Maximum cross-sectional area
C_{D_β}	Pressure drag coefficient of a boattail = D_β/qA_m
C_{p_b}	Base pressure coefficient = $\frac{p_b - p_\infty}{q}$
d_b	Base diameter
d_j	Jet exit diameter
d_m	Maximum diameter
p_b	Base pressure
p_∞	Free-stream static pressure
q	Free-stream dynamic pressure
β	Terminal angle of boattail

ABSTRACT

The results of the afterbody drag study are presented in four volumes--Volume 1: Drag of Conical and Circular Arc Afterbodies; Volume 2: Jet Interference Effects on Subsonic Boattail Drag; Volume 3: Literature Survey; and Volume 4: Data and Analysis.

Volume 1 includes a series of charts that enable the drag of conical and circular arc afterbodies without jet flow to be determined.

ADMINISTRATIVE INFORMATION

The work reported was performed for the David W. Taylor Naval Ship Research and Development Center by Payne, Incorporated under ONR Contract N00014-77-C-0039 as part of an evaluation of afterbody drag. The afterbody drag project was supported by the Naval Air Systems Command and the Naval Weapons Center under Program Elements 63361N, 62332N, and 62241N; Task Areas W15X20000, F32.322.203, and WF41.421.201; and Work Units 1660-234 and 1660-235.

The figures are in the format of Payne, Incorporated.

INTRODUCTION

Aerodynamic drag is one of the major factors to be considered when attempting to predict airborne vehicle performance. Although there are sources of aerodynamic drag, such as wings, fuselage, nose, and tails, the afterbody drag of the fuselage is usually the most difficult to evaluate. Inasmuch as some vehicles develop 30 percent of their zero-lift drag from the afterbody, an accurate method for predicting the magnitude of this drag is needed.

Afterbodies as a rule are tapered, or boattailed, in some manner. These afterbodies suffer from skin friction drag, base drag, and pressure drag. As air flows over the junction of the forebody and the boattail, a low pressure peak is developed. As the flow continues downstream the pressure rises, depending upon the boattail length and curvature. In some cases the pressure can exceed that of the free stream. For most practical shapes, however, the pressure distribution over the boattail results in a pressure drag. Even though the tapered afterbody develops a pressure drag,

its overall effect is less total afterbody drag. This is because the taper both reduces the base area and increases the pressure on the aft-facing base such that the base drag is appreciably reduced.

The results of the afterbody drag study performed at DTNSRDC are presented in four volumes:

Volume 1 - Drag of Conical and Circular Arc Afterbodies without Jet Flow

Volume 2 - Jet Interference Effects on Subsonic Boattail Drag

Volume 3 - Literature Survey

Volume 4 - Data and Analysis

The objective of the phase of the study presented in Volume 1 is to establish a data base of afterbody drag charts based on data from the numerous references (608) listed in Volume 3.

STATE OF THE ART

A survey of the afterbody drag literature disclosed that the vast majority of available reports on experiments related to the subject were quite specialized, treating nonbasic specific configurations, and were not suitable for establishing a broad basis from which the effects of the various geometrical, physical, and environmental parameters could be systemmatically investigated. Only a small number of reports were suitable for this purpose. The widest range of useful reports were for conical afterbodies in the subsonic and transonic range; however, a number of reports on systematic investigations of nonconical afterbodies (such as circular arc) were also useful.

The surveyed reports are in three groups: (1) experimental data, (2) empirical and semiempirical methods of correlation, and (3) theoretical models of the flow. Only a small number of reports in the first group were suitable for the correlation of boattail drag and base pressure coefficients as a function of the geometric parameters of the boattail. Those reports most valuable were References 1 through 10.* In the second group, four different approaches were considered. These approaches were proposed in References 11, 12 and 13, 14 and 15, and 16.

*A complete listing of references is given on page 51.

McDonald and Hughes[11] proposed a method for a correlative prediction of boattail and base drag of parabolic, circular arc, and conical afterbodies including the effect of jet flow on the drag characteristics of the three types of afterbodies. However, the method does not consider variation of the drag characteristics with Mach number. The variation with Mach number, even in the subsonic range from Mach number 0.6 to 0.9, can be considerable. There are also other restrictions in the use of the method. McDonald and Hughes[11] base their correlation method on the finding that there is a unique relationship between the base pressure and the boattail drag, and that this relationship is essentially linear over the greater part of the base pressure range. This finding appears to be confirmed by Kurn.[8] Furthermore, McDonald and Hughes[11] found that if the three afterbody shapes have identical afterbody angles β at the base and identical base diameter ratios d_b/d_m, the boattail drag coefficients are approximately the same, and the base pressure coefficients are approximately the same for the circular arc and the parabola.

According to the present investigation, the McDonald and Hughes[11] finding in regard to the boattail drag appears to be confirmed in the Mach number range from 0.6 to 0.8, considering the uncertainties of the data. However, for Mach numbers of 0.9 and higher, the boattail drag curves for conical and circular arc afterbodies in the present investigation appear to be quite different.

Bergman[12] presents a qualitative and quantitative analysis of the effect of nozzle geometry and some physical parameters on the boattail drag. However, base drag and the effect of Mach number are not considered. A subsequently proposed method by Kurn[8] also does not consider base drag and is suggested only for Mach numbers less than 0.9. The latter approach corrects a "basic drag," which is a boattail drag with a cylindrical sting, for the jet effects of the actual plume shape and the entrainment. The advantage of this approach is that if the basic drag of the boattail with a cylindrical sting can be evaluated with sufficient accuracy on a parametric basis, the corrections for the plume shape and entrainment effects may be significantly smaller than in the no-sting case. The method is applicable in the jet-on case for afterbodies with no base area.

The method of Swavely and Soileau[14] uses a parameter IMS (Integral Mean Slope) which is obtained by integrating an area ratio equation:

$$IMS = \frac{\int_{(A_j/A_m)}^{1.0} \frac{d\,(A/A_m)}{d\,(X/d_{eq})}\, d\,(A/A_m)}{1 - (A_j/A_m)}$$

where

$$d_{eq} = \left(\frac{4\,A_m}{\pi}\right)^{1/2}$$

Thus, the parameter IMS is obtained from the boattail and nozzle geometry as a function of the area ratios and the axial coordinate from the maximum cross-sectional area point aft. The method was designed for arbitrary and complex afterbody shapes including twin jets. However, as shown by Brazier and Ball,[15] the method failed for configurations whose area plots involved regions of steep slopes aft of the point where separation occurs. To correct this problem, an IMS_T (Integral Mean Slope-Truncated) approach was introduced. This approach is based on specifying a maximum slope of the nondimensional area distribution which can be used in the IMS calculation. The specified maximum slope is substituted for the real slope at each step of the IMS calculation for which the real slope exceeds the maximum. Even with this improvement, Brazier and Ball[15] urge extreme caution in predicting nozzle and afterbody drag from data obtained with a "representative" forebody to a forebody of arbitrary shape and length; see Effect of Reynolds Number, page 11. The method apparently is applicable to subsonic flight and is limited to configurations with negligible annular base area.

The prediction method of Presz and Pitkin,[16] which is applicable to the subsonic case, requires extensive computations. The method predicts

the flow separation point and pressure distribution on a boattail with a given solid surface sting in subsonic flow. After determination of the flow separation point, an iterative method is used to match a calculated inviscid flow field, an attached boundary layer, a control volume separation point, and the separated flow field model. The pressure distribution obtained then may be integrated to give the boattail pressure drag coefficient. The method does not consider base drag and effects of jet plume shape and entrainment.

The four methods presented are considered to be representative of the approaches proposed for the solution of the afterbody drag prediction problem in the subsonic and transonic range. The methods, as reported in the references, show correlations for some specific conditions, boattail configurations, and Mach numbers. The prediction reliability for other conditions, configurations, and Mach numbers has not been estimated.

With respect to supersonic afterbody drag, theory is of greater applicability because supersonic flow is easier to treat mathematically. Consequently, a number of mathematical treatments of afterbody drag in supersonic flow are available. Although the supersonic case beyond M = 1.3 was not considered in this investigation, the work of Chapman,[17] with respect to base pressure, is fundamental. A correlation based on the Chapman method for a variety of configurations and local Mach numbers is discussed by Love.[18] The base pressure is also useful in determining the boattail drag coefficient in the supersonic case. A substantial amount of material is available to allow a systematic treatment of boattail and base drag.[19-22] An evaluation of the methods presented in References 19 through 22 has been made by King.[23]

DISCUSSION

AFTERBODY GEOMETRY

A conical boattail is completely defined by the boattail angle β and the diameter ratio d_b/d_m:

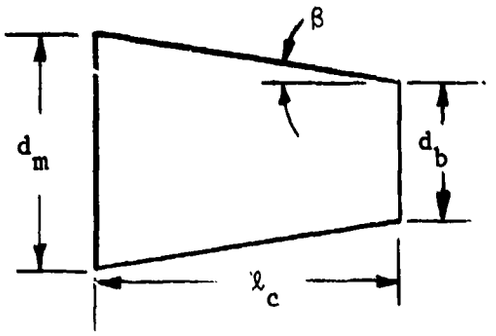

Conical

A nonconical afterbody may involve any kind of curvature of the boattail. The number of parameters defining these boattails is generally larger than two, unless the forebody is tangent to a circular arc afterbody. McDonald and Hughes[11] and Reid and Hastings[24] indicate that the most important parameter besides the diameter ratio is the boattail angle at the base - β.

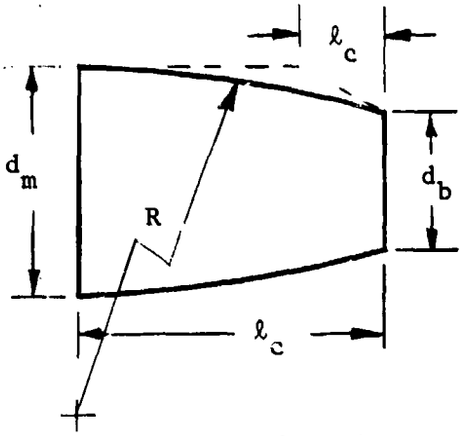

Circular Arc

The relationship among the parameters β, d_b/d_m, and ℓ/d_m is shown in Figure 1 for conical afterbodies and in Figure 2 for the circular arc afterbodies.

DRAG OF CONICAL AFTERBODIES

Boattail Drag

Experimental data used for correlation of conical boattail drag shown in Figure 3 were taken from References 1 and 2. Data from other sources were also considered, but are not included in this correlation. The no-jet flow experimental data of Cubbage[1] displayed a very systematic, consistent, and reasonable behavior with very few exceptions. Furthermore, the data were in good agreement with the experimental data of Silhan and Cubbage,[2] which was independently considered by other investigators to contain very

reliable data.[25] Values of boattail drag coefficients from other sources generally tended to be higher than those from References 1 and 2 and introduced only a scatter of the data points. The experiments reported in References 1 and 2 were performed at Mach numbers from 0.6 to 1.28 (1.3), and with conical afterbodies having boattail angles β = 3.0, 5.6, 8.0, 16.0, 30.0, and 45.0 deg. The diameter ratio d_b/d_m of the experimental models was 0, 0.55, 0.7, and 0.85. The afterbodies of Reference 1 had annular base areas with d_j/d_b = 0.65 and 0.75. Data taken from Reference 2 were for open base areas.

Figure 3 shows the boattail pressure drag coefficient C_{D_β} as a function of β and $(d_b/d_m)^2$. The particular form of presentation was chosen because of ease of interpolation during use of the graphs. The graphs were obtained by cross plotting for each Mach number graphs of the type shown in Figure 4. The data points in Figure 4 were obtained from Reference 1 (jet-off case) and from Reference 2, which had a model with a solid flat base and no nozzle provisions. Only values of β up to 16 deg were used.

There is a noticeable change in the character of the constant β curves in Figure 3 as well as the C_{D_β} values themselves between Mach numbers 0.6 and 0.9. The trend continues in the supersonic range, although after M = 1.1, the relative values of the C_{D_β} are decreasing as would be expected. The change of C_{D_β} values between Mach numbers 0.6 and 0.9 is particularly significant for the lower $(d_b/d_m)^2$ ratios and $\beta > 8$ deg. Note that in the supersonic case, the C_{D_β} values continue to increase as the $(d_b/d_m)^2$ ratio approaches zero. This is in contrast with the circular arc afterbodies, in which case the boattail pressure coefficient C_{D_β} reaches maximum values somewhere between $0 < (d_b/d_m)^2 < 1.0$.

Base Drag

Figure 5 presents the base pressure coefficient C_{p_b} as a function of β and $(d_b/d_m)^2$ at the same Mach numbers from 0.6 to 1.3. Data in Figure 5 were taken from References 1 and 3. There was generally a systematic, consistent, and reasonable agreement between the data from the two references with a small number of exceptions. Data from Reference 3 were taken for the open base configuration. The average difference in base drag

coefficient between an open base and a flat base conical afterbody is about 0.01, according to the experiments of Reference 3, with the flat base giving a higher base drag coefficient. According to Cubbage and Andrews[5] and Kurn,[8] the variation of base pressure over the drag-producing base area in a radial direction is fairly insensitive for the jet-off case, although some variation usually does occur in the jet-on case. The base drag coefficients in Reference 1 were computed using pressure measurements at the base annulus only, while the same coefficients in Reference 3 were computed from pressure measurements at the open base.

The graphs in Figure 5 were obtained by the following method. When the base pressure coefficient C_{p_b} was plotted against $(d_b/d_m)^2$ for constant values of β, it was noted that the resulting behavior of the constant β points was very regular and consistent at all Mach numbers. In fact, whenever three points for the β were available at different $(d_b/d_m)^2$ ratios, the trend of the C_{p_b} curves as a function of $(d_b/d_m)^2$ was generally linear. Consequently, it was assumed that for $(d_b/d_m)^2 > 0.1$, C_{p_b} is essentially a linear function of $(d_b/d_m)^2$. In the vicinity of $(d_b/d_m)^2 = 1.0$ it was assumed that the C_{p_b} converges to the value of C_{p_b} for a cylindrical afterbody. The basic pattern occurred consistently at all Mach numbers from 0.6 to 1.3 for data from References 1 and 3. Moreover, data from Reference 1 was for an annular base with $d_j/d_b \simeq 1$. Data from Reference 2 and Reference 1 at $d_j/d_b = 0.65$ did not generally follow this consistent pattern and were not used for establishing the correlation; however, data from Reference 1 for $d_j/d_b = 0.65$ are shown in Figure 6 at some angles of β, e.g., $\beta = 5.6$ and 16 deg. Note that with respect to the boattail drag coefficient, the agreement between References 1 and 2 was generally very good, being consistent at all Mach numbers of the experiments.

The base pressure coefficients for a cylinder were chosen from the available published data at the respective Mach numbers to correlate with the experimental data used in the present investigation. These data and the C_{p_b} values for a cylindrical afterbody used in the present correlation are shown in Figure 7. Because the mean value of the $(d_b/d_m)^2$ ratios used in the correlation was in the vicinity of 0.6, which also represents a significant point in practical applications, $(d_b/d_m)^2 = 0.6$ was chosen as a reference point in the graphs of the type shown in

Figure 6. The slope $\partial(C_{p_b})/\partial(d_b/d_m)^2$ and the C_{p_b} values from the dashed lines at $(d_b/d_m)^2 = 0.6$ were plotted versus β as shown in Figure 7, and the C_{p_b} and the slope curves were fitted through the data points. The resulting slopes and C_{p_b} values were superimposed on Figure 6 from which Figure 5 was obtained by cross-plotting C_{p_b} as a function of β for constant $(d_b/d_m)^2$ values. The general character of the correlation shown in Figure 6 was typical for all Mach numbers.

DRAG OF CIRCULAR ARC AFTERBODIES

Boattail Drag

Experimental data for the correlation of circular arc boattail drag were taken from References 2, 8, 9, and 10. Reference 2 provides systematic experimental data for circular arc afterbodies as well as conical afterbodies. As mentioned, the conical afterbody experimental data of Reference 1 showed an exceptionally good agreement with the corresponding data from Reference 2. It would be reasonable to expect the same reliability with respect to the circular arc experimental data of Reference 2, particularly in view of the evaluation by others[25] of the reliability of the data contained in Reference 2. Moreover, there is also a reasonably good agreement of the circular arc boattail drag between Reference 2 and References 8, 9, and 10. In comparable cases, there was also quite good agreement with the data from unpublished DTNSRDC experiments. Experiments reported in Reference 2 were performed at Mach numbers from 0.6 to 1.3 for solid flat base circular arc boattails with boattail angles β = 0, 3, 5.6, 8, 16, and 45 deg and d_b/d_m ratios of 0, 0.55, 0.7, and 0.85. Experiments reported in Referen e 10 had circular arc boattails with boattail angles of 15.8, 27.5, and 34 deg and substantially open base areas. In addition, test results of a circular arc reference nozzle with a boattail angle of 21.57 deg were also included. Experiments reported in Reference 9 had circular arc boattails with β = 8.3, 11, 14.8, 16.5, and 22.1 deg. Experiments reported in Reference 8 were performed with a tangent ogive and progressively truncated versions of it with boattail angles of 4.4, 9.6, 14.6, and 17.1 deg.

Figure 8 shows the boattail pressure drag coefficient C_{D_β} as a function of β and $(d_b/d_m)^2$. The typical graph shown in Figure 9 was obtained by fairing curves through C_{D_β} values for constant d_b/d_m ratios using data from References 2, 8, 9, and 10. Figure 8 was then obtained by cross-plotting C_{D_β} values for constant boattail angles β from Figure 9. Thus, for each β curve in Figure 8, five points (at five d_b/d_m values) were available. Additional experimental data for d_b/d_m values other than 0, 0.55, 0.7, and 0.85 were used to check the correlation.

A major characteristic of Figure 9 is the steep drag rise at about 8-deg boattail angle. This steep drag rise for the $d_b/d_m = 0.85$ case, which is particularly distinctive for M = 1.0 and 1.1 shown in Figures 8(d) and 8(e), accounts for the characteristic increase of C_{D_β} at $\beta = 8$ deg and $d_b/d_m = 0.85$ shown in Figure 9. Because this characteristic occurred consistently at all Mach numbers from 0.8 to 1.3, it could not be regarded as an experimental error.

In comparing the C_{D_β} curves for circular arc afterbodies with the C_{D_β} curves for conical afterbodies, the main difference is in the character of the boattail pressure drag for $(d_b/d_m)^2$ ratios of less than about 0.3 to 0.5. While in the supersonic case, the C_{D_β} values for the conical boattails continue to rise at these d_b/d_m ratios, the corresponding C_{D_β} values for the circular arc boattails exhibit a clear tendency to decrease with decreasing d_b/d_m ratios.

For $(d_b/d_m)^2$ ratios approaching 1.0, the boundary of the maximum C_{D_β} values is approximately the same for both the conical and circular arc boattails at the higher Mach numbers investigated. With increasing boattail angles and decreasing d_b/d_m ratios, however, the circular arc boattail is definitely more advantageous.

Base Drag

Figure 10 presents the base pressure coefficient C_{P_b} as a function of β and $(d_b/d_m)^2$ at Mach numbers from 0.6 to 1.3. Data in Figure 10 were taken from References 2, 8, 9, and 10. The experimental models of References 2 and 8 had solid flat bases. The models of References 9 and 10 had open bases with very small annular base areas.

The graphs in Figure 10 were obtained by a similar method used to obtain the base pres. res for the conical afterbody. However, some of the slopes of the base pressure coefficient C_{p_b} as a function of boattail angle β could not be obtained directly for lack of suitable data. Consequently, some of the data points shown in Figure 12 do not represent actual experimental values but are extrapolations of available data. The data points and the correlation curves for a typical case are shown in Figure 11. As in the conical case, it was assumed that within the larger part of the $(d_b/d_m)^2$ range, the base pressure coefficient C_{p_b} is essentially a linear function of $(d_b/d_m)^2$. This assumption appears to be justified on the basis of available data. The correlation shown in Figures 11 and 12 is typical for all investigated Mach numbers.

One notable difference between the graphs of Figure 10 for the circular arc afterbodies and the graphs of Figure 5 for the conical afterbodies is that the sensitivity of the base pressure coefficient C_{p_b} with β in the lower β range is much more pronounced in the circular arc case. This may partly explain the increased scatter of experimental data for the circular arc afterbodies in the lower β range. The base pressure apparently may experience large variations with relatively small variations in model geometry.

Another characteristic of the base pressure coefficient for circular arc afterbodies is the apparent movement of the optimum boattail angle β from the vicinity of 24 deg at Mach number 0.6 to the vicinity of 16 deg for the supersonic case.

CIRCULAR ARC-CONICAL AFTERBODY COMBINATIONS

The effect of rounding off the corner at the cone-cylinder juncture of a basic conical boattail is generally beneficial, particularly if the round-off radius is larger than $2d_m$. This effect for a 15-deg conical boattail is reported in Reference 26.

In using Reference 26, it must be considered that the experiments have been performed and reported for sting-supported wind tunnel models. The effect of the sting may be evaluated from the information contained in Reference 7.

EFFECT OF REYNOLDS NUMBER

The results of this investigation have been presented under the assumption that the effect of Reynolds number may be ignored. This may be justified for preliminary design purposes in view of the present knowledge of this subject. The following discussion of the effect of Reynolds number pertains only to turbulent boundary layers within the subsonic and transonic Mach number range.

There appears to be some inconsistency in the published reports regarding the evaluation of the effects of Reynolds number on afterbody drag characteristics. Reference 27 presents data which show an extremely large dependency of boattail drag on Reynolds number. Conversely, Reference 28 shows that for practical purposes there is no effect of Reynolds number on the boattail drag of afterbodies. However, there exist significant differences between the conditions of the experiments reported in the two references. These differences may be reviewed in the light of the information and discussions contained in References 29 and 30. The results reported in Reference 27 were obtained from wind tunnel and flight tests. The afterbodies were tested as part of an aircraft configuration in a very complex flow field. Furthermore, most of the flight data were taken while in coordinated turns under an angle of attack and with load factors up to 2.5 g's.

Conversely, the results reported in Reference 28 were obtained only from wind tunnel experiments with sting-mounted, cone-cylinder-afterbody models. Models of similar configurations were also tested in the experiments reported in Reference 29. Although the three models tested in the experiment reported in Reference 29 showed some effect of Reynolds number, the effect on all the models was not consistent and, in any case, did not show the extreme drag variation with Reynolds number reported in Reference 27. Perhaps the most important conclusion of the report is that the absolute level of afterbody pressure drag can vary due to experimental factors such as tunnel characteristics and model installation. The same conclusion can be applied to flight tests. Also, changing the Reynolds number may alter the tunnel characteristics and, therefore, it may become difficult to isolate the two effects.

Reference 30 shows that the forebody configuration strongly influences the drag characteristics of the afterbody and vice versa. The report also concludes that the same afterbody tested as an isolated halfbody either in different wind tunnels or in the same tunnel with a different blockage will give very different afterbody drag values.

Conclusions based on the totality of the four reports are:

1. The effect, if any, of Reynolds number on afterbody drag for preliminary design purposes cannot be determined with any reliability.

2. The effect of Reynolds number on a specific configuration which includes afterbody must be determined for that particular configuration as a whole and not as a sum of the effects on the separate parts of the configuration.

SUMMARY

For smaller boattail angles β the boattail drag coefficient is relatively invariant with Mach numbers up to 0.9. At M = 1, an increase of the value of C_{D_β} plots show a marked regularity for Mach numbers below 0.9 and above 1.0, while the plots for M = 0.9 and 1.0 reflect the changes occurring in the flow regime in this transonic range.

At subsonic speeds, C_{D_β} is decreasing with decreasing $(d_b/d_m)^2$ ratio from a maximum at about $(d_b/d_m)^2 = 0.5$, suggesting a pressure recovery on the boattail. However, at supersonic speeds, such pressure recovery apparently does not occur.

The effect of boattailing on the base pressure is very apparent. At M = 0.6, C_{p_b} is continuously increasing with increasing β and with decreasing $(d_b/d_m)^2$. However, already at M = 0.8, a marked change in the behavior of the base pressure starts to occur at β above approximately 10 deg. This behavior of the base pressure coefficient continues throughout the investigated range of Mach numbers above 0.6. Also, the effect of the $(d_b/d_m)^2$ in this transonic range becomes very noticeable, particularly at M = 1.0 and 1.1. The large positive base pressure coefficient is quite pronounced for boattail angles of around 12 deg. However, above M = 1.0, the area of positive pressure coefficient is shrinking quite noticeably with increasing Mach number.

The correlation in this investigation has been obtained assuming a turbulent boundary layer and a negligible effect of Reynolds number. This assumption appears to be justified in view of recent experiments.[15]

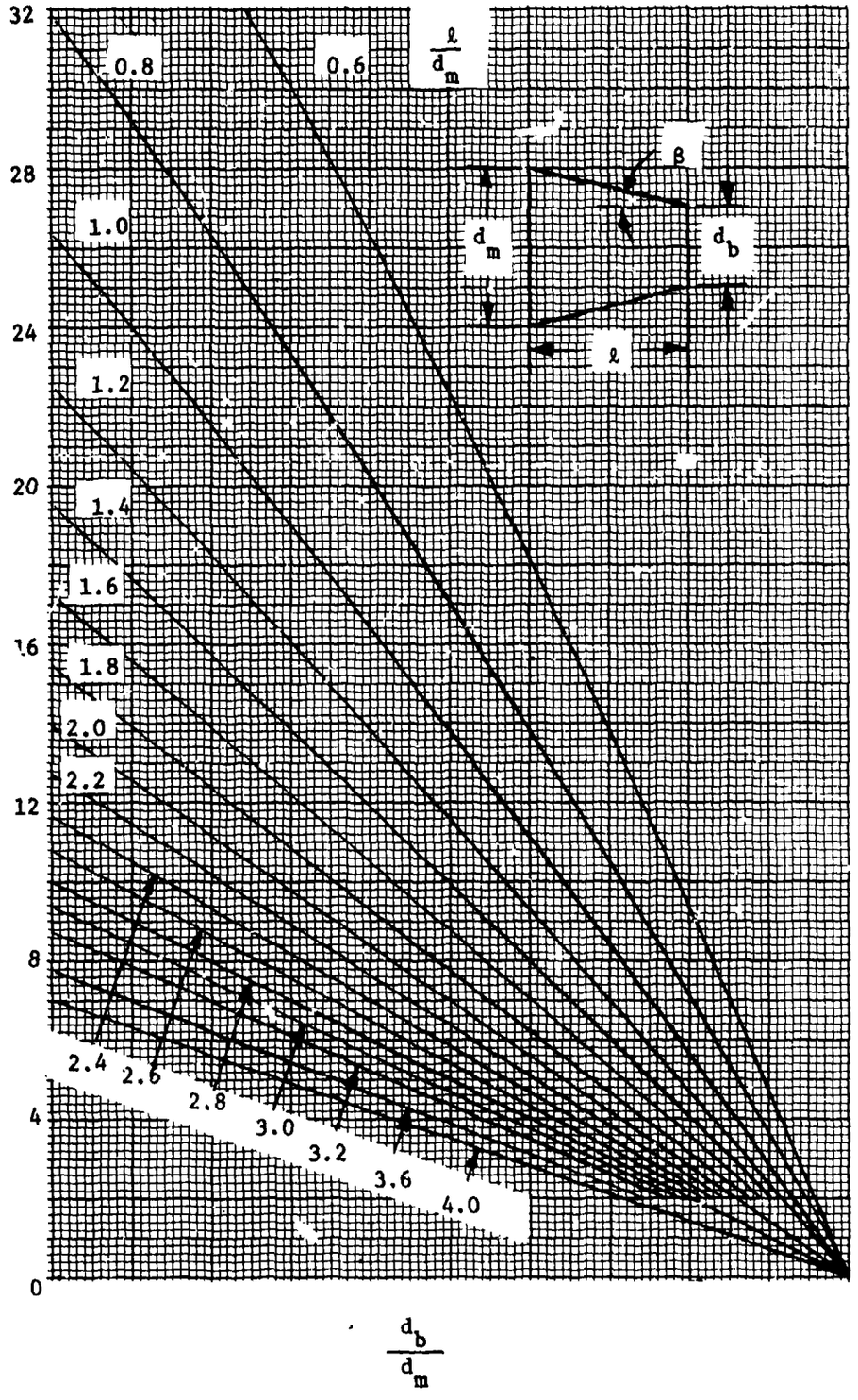

Figure 1 - Dimensionless Geometric Characteristics of Conical Boattails

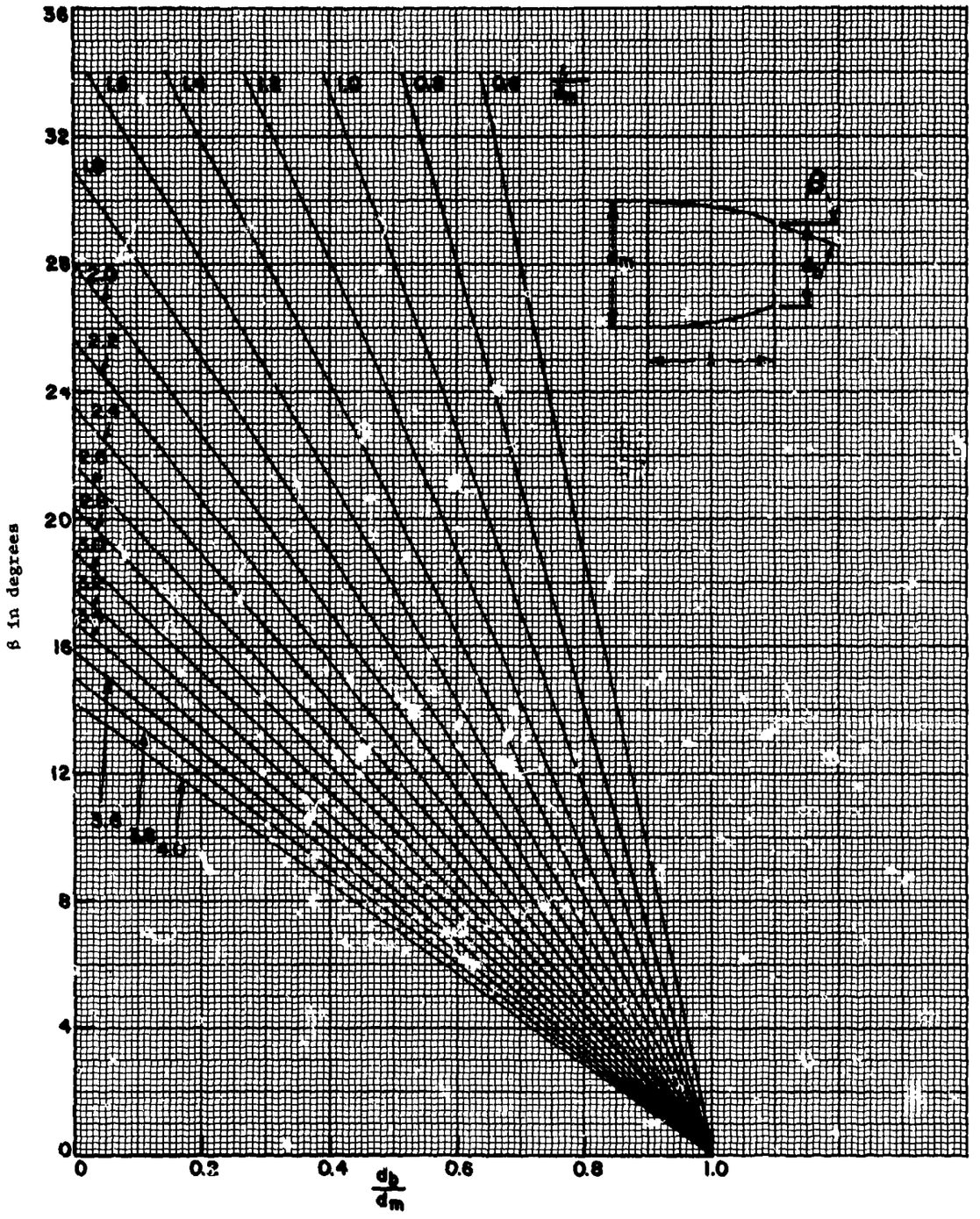

Figure 2 - Dimensionless Geometric Characteristics of Tangent Circular Arc Boattails

Figure 3 - Conical Boattail Drag Coefficient with Jet Off

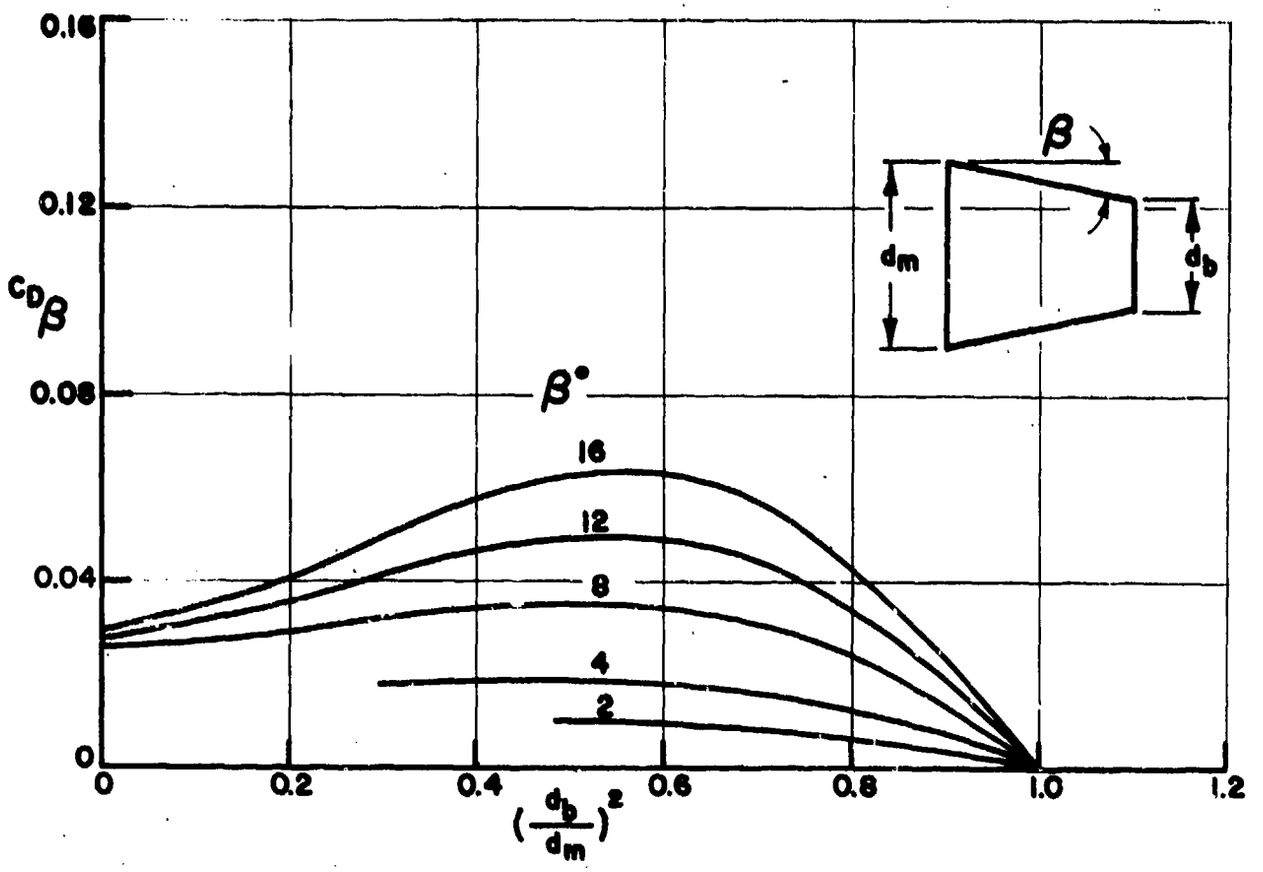

Figure 3a - M = 0.6

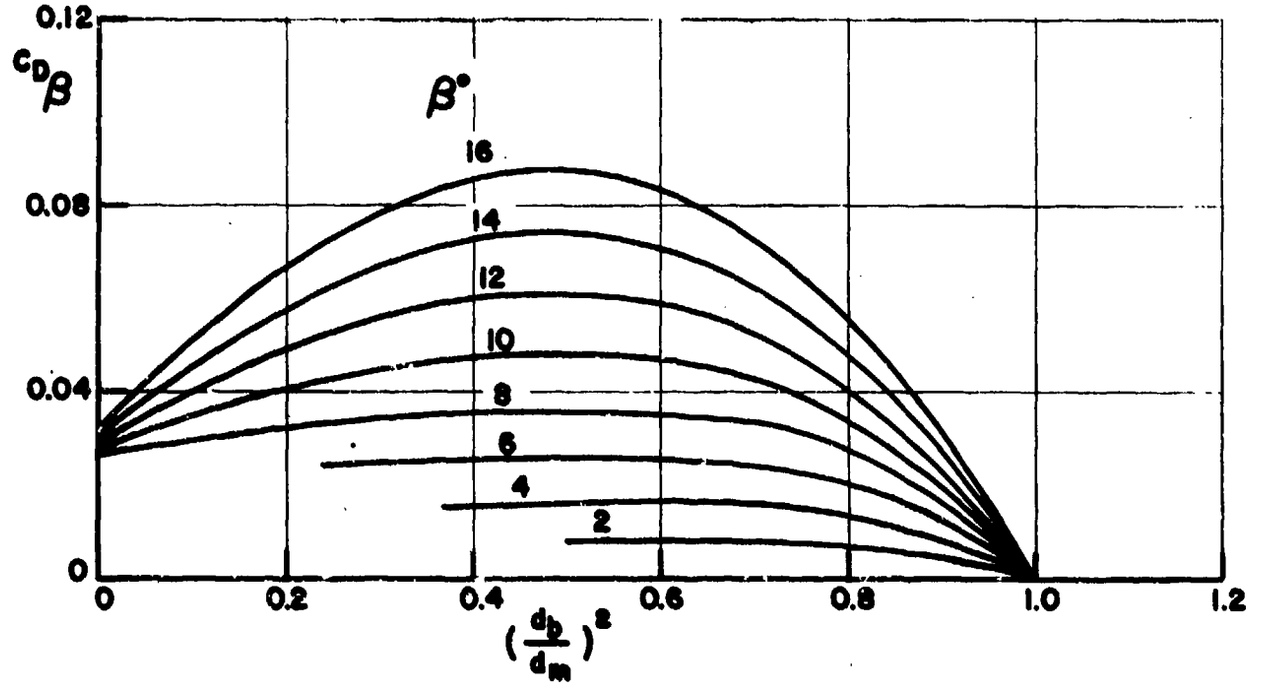

Figure 3b - M = 0.8

Figure 3 - Continued

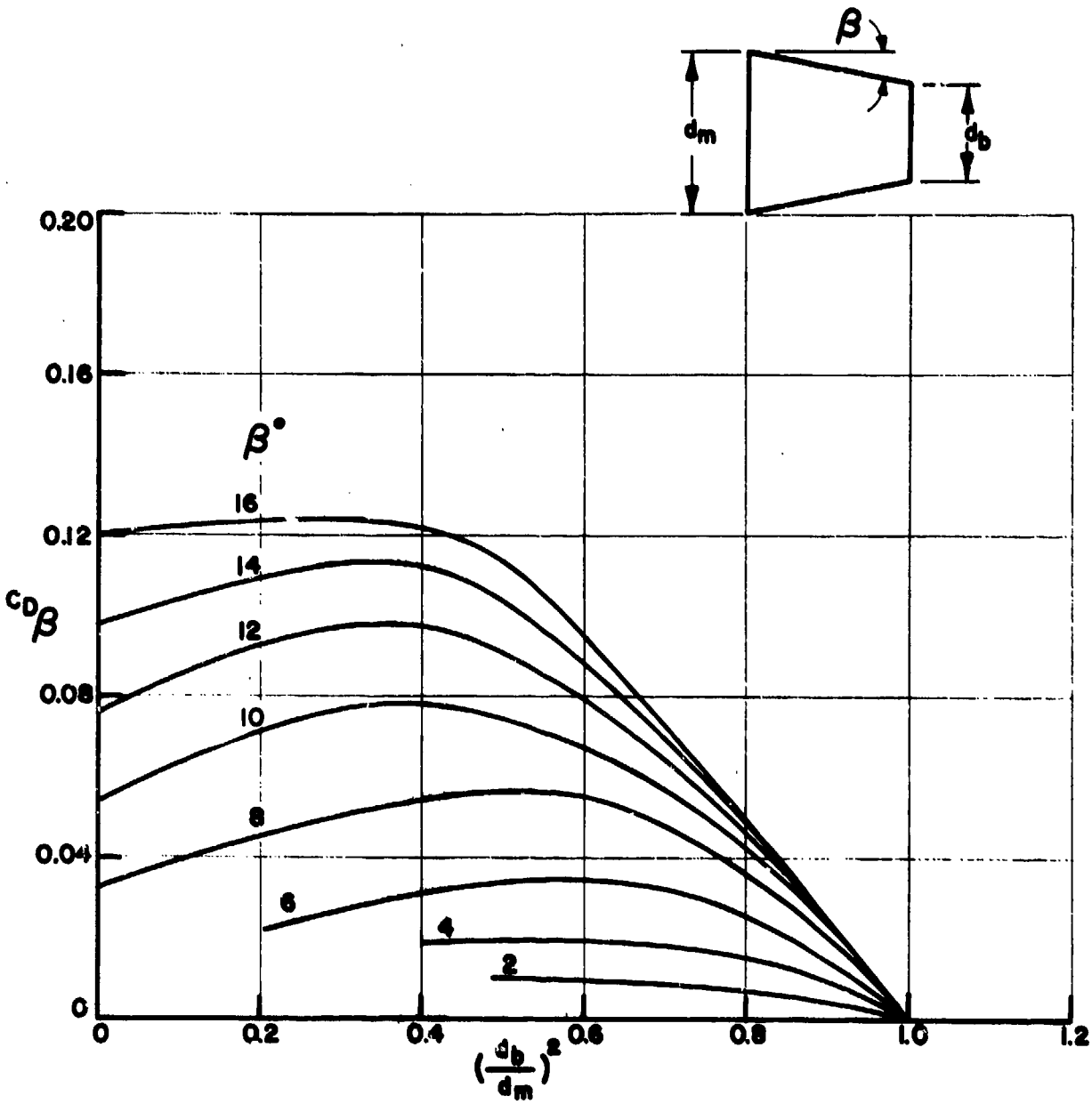

Figure 3c - M = 0.9

Figure 3 - Continued

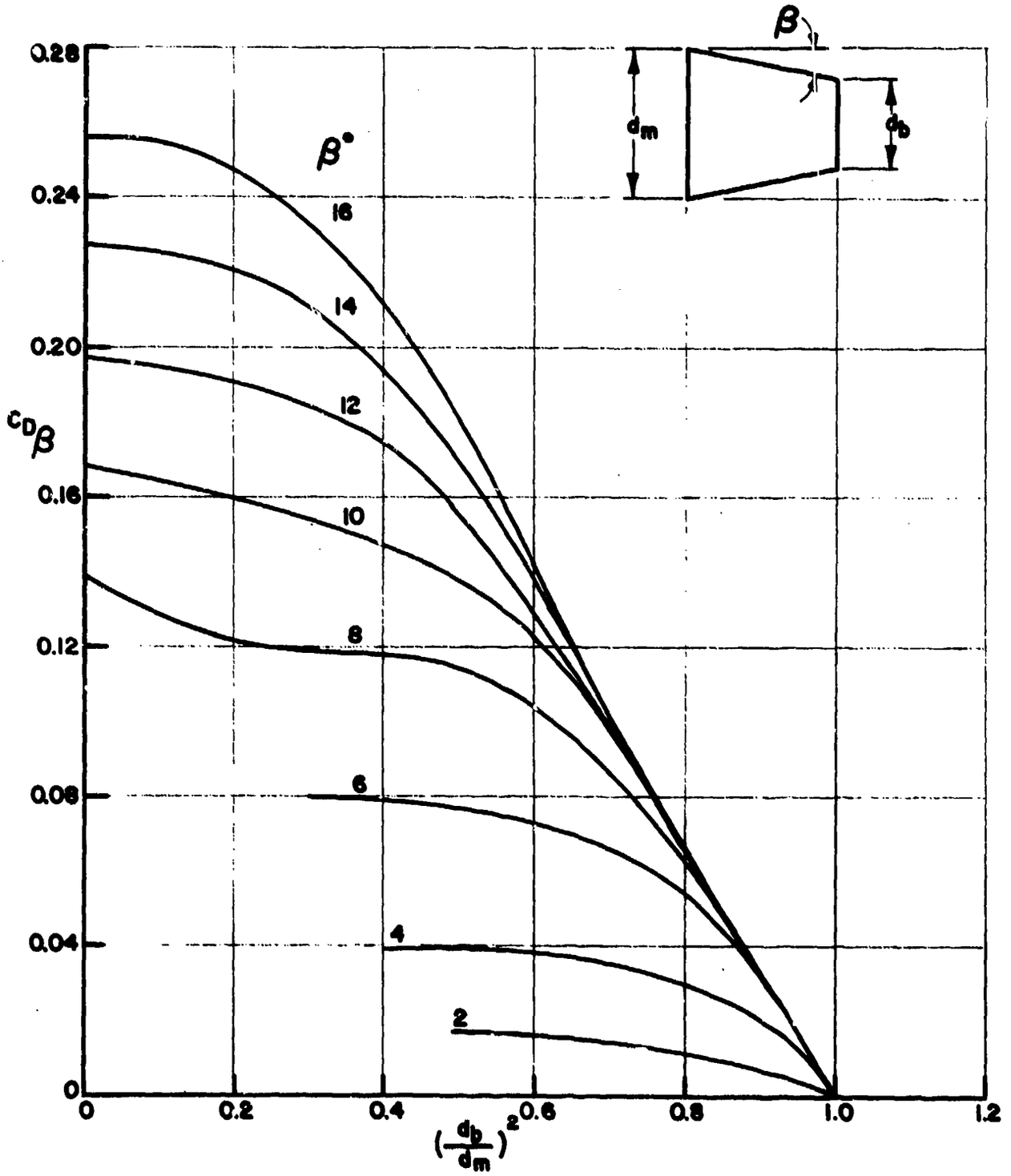

Figure 3d - M = 1.0

Figure 3 - Continued

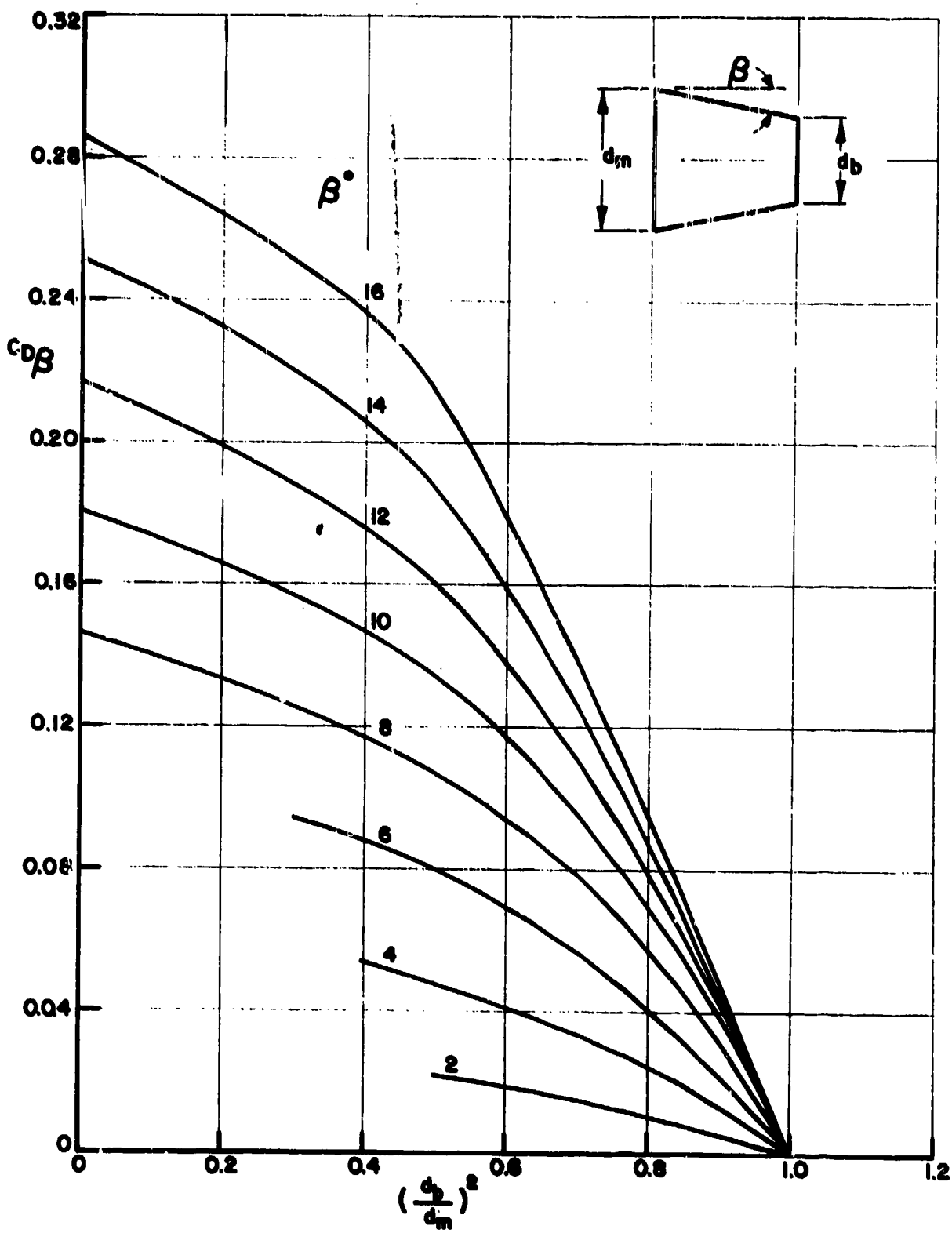

Figure 3e - M = 1.1

Figure 3 - Continued

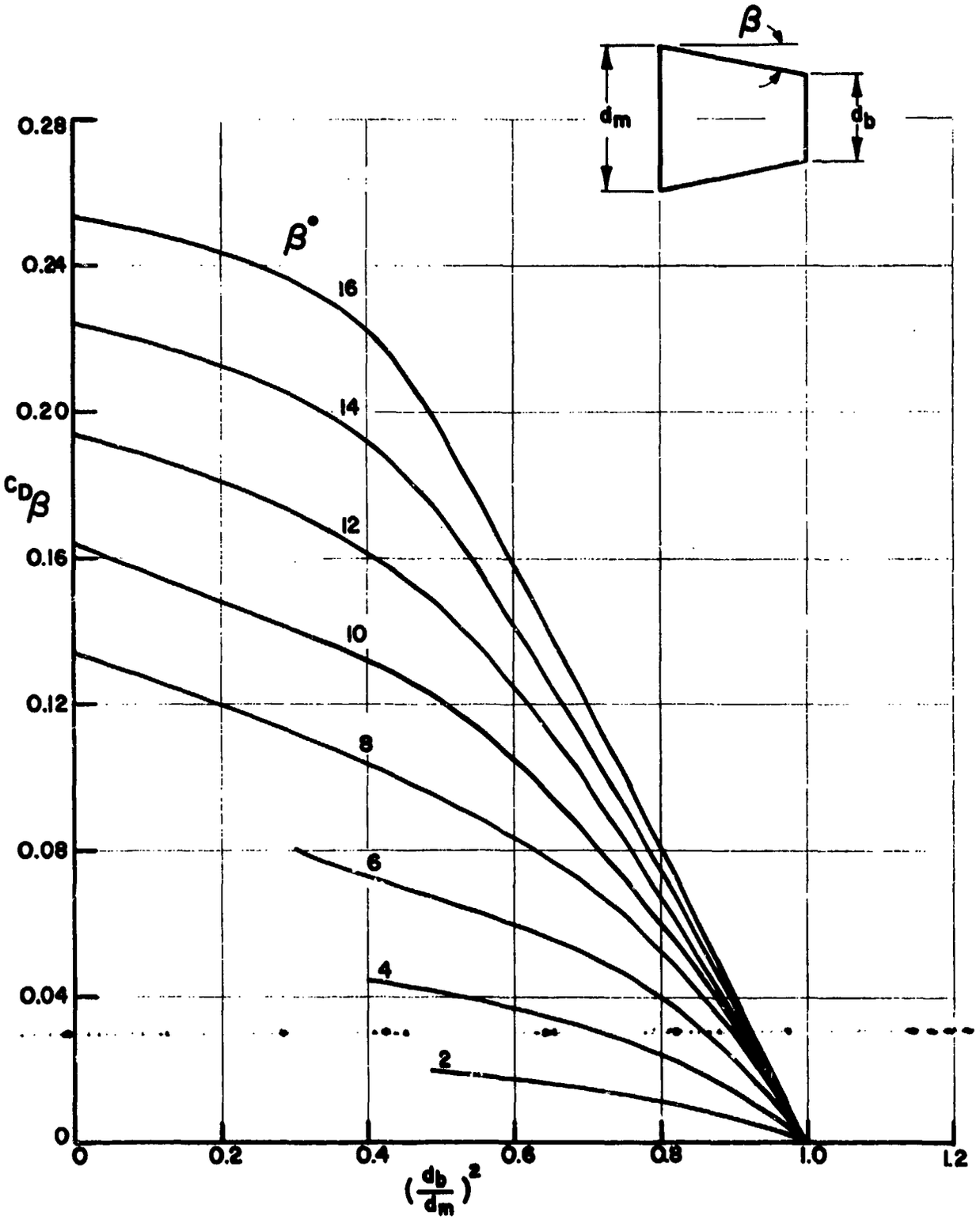

Figure 3f - M = 1.2

Figure 3 - Continued

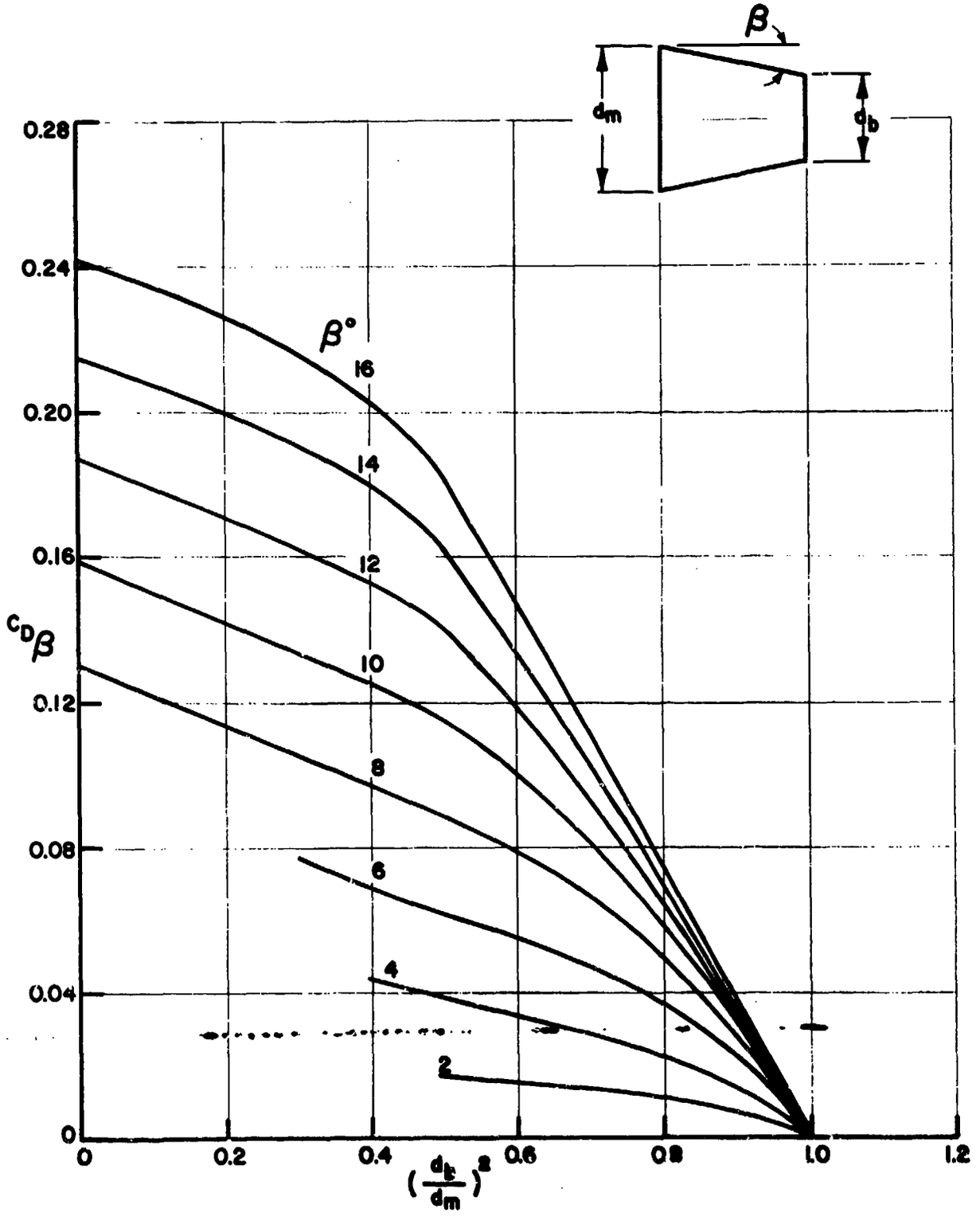

Figure 3g - M = 1.3

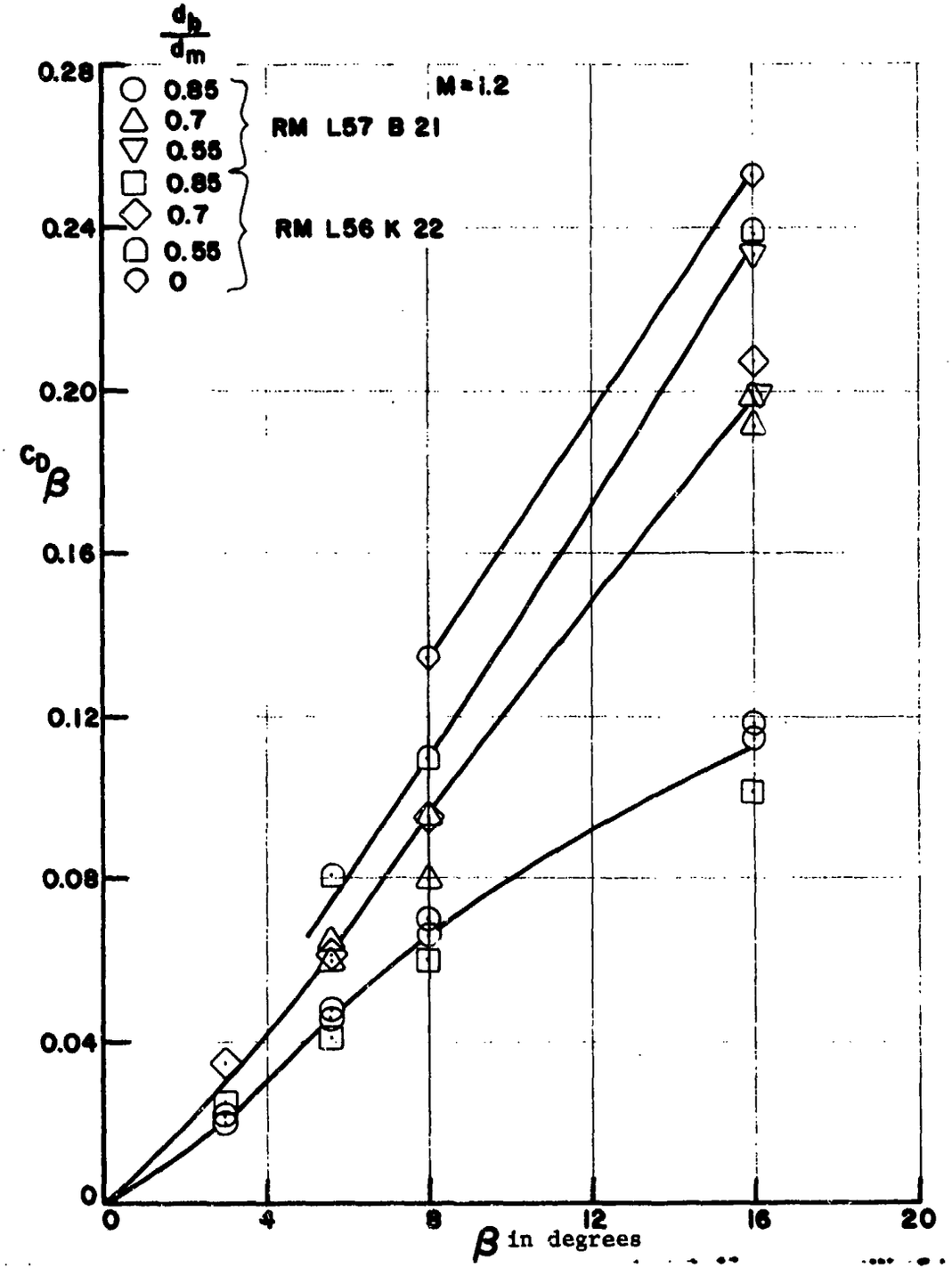

Figure 4 - A Correlation of Conical Boattail Drag Coefficients with Jet Off

Figure 5 - Conical Boattail Base Pressure Coefficients with Jet Off

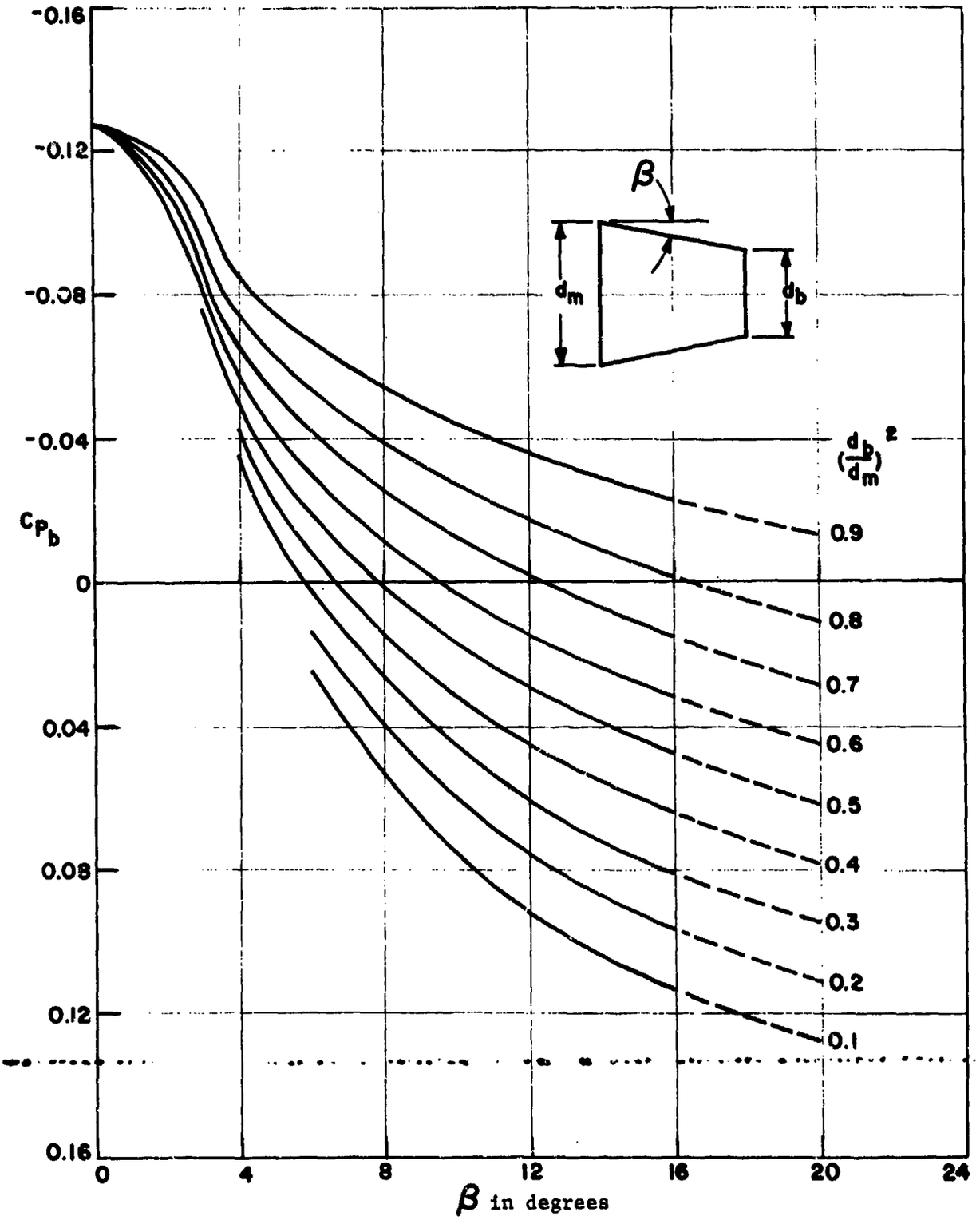

Figure 5a - M = 0.6

Figure 5 - Continued

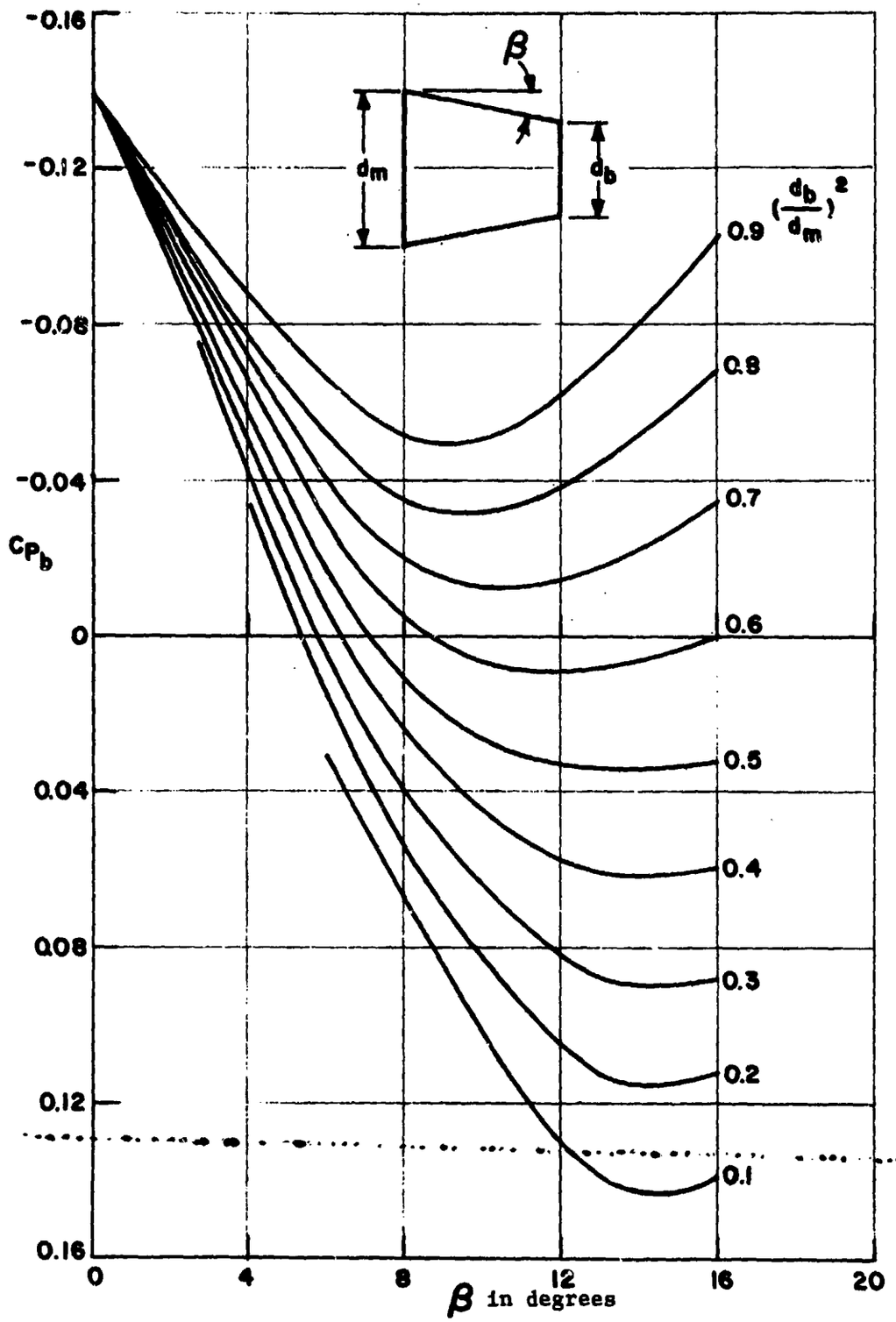

Figure 5b - M = 0.8

Figure 5 - Continued

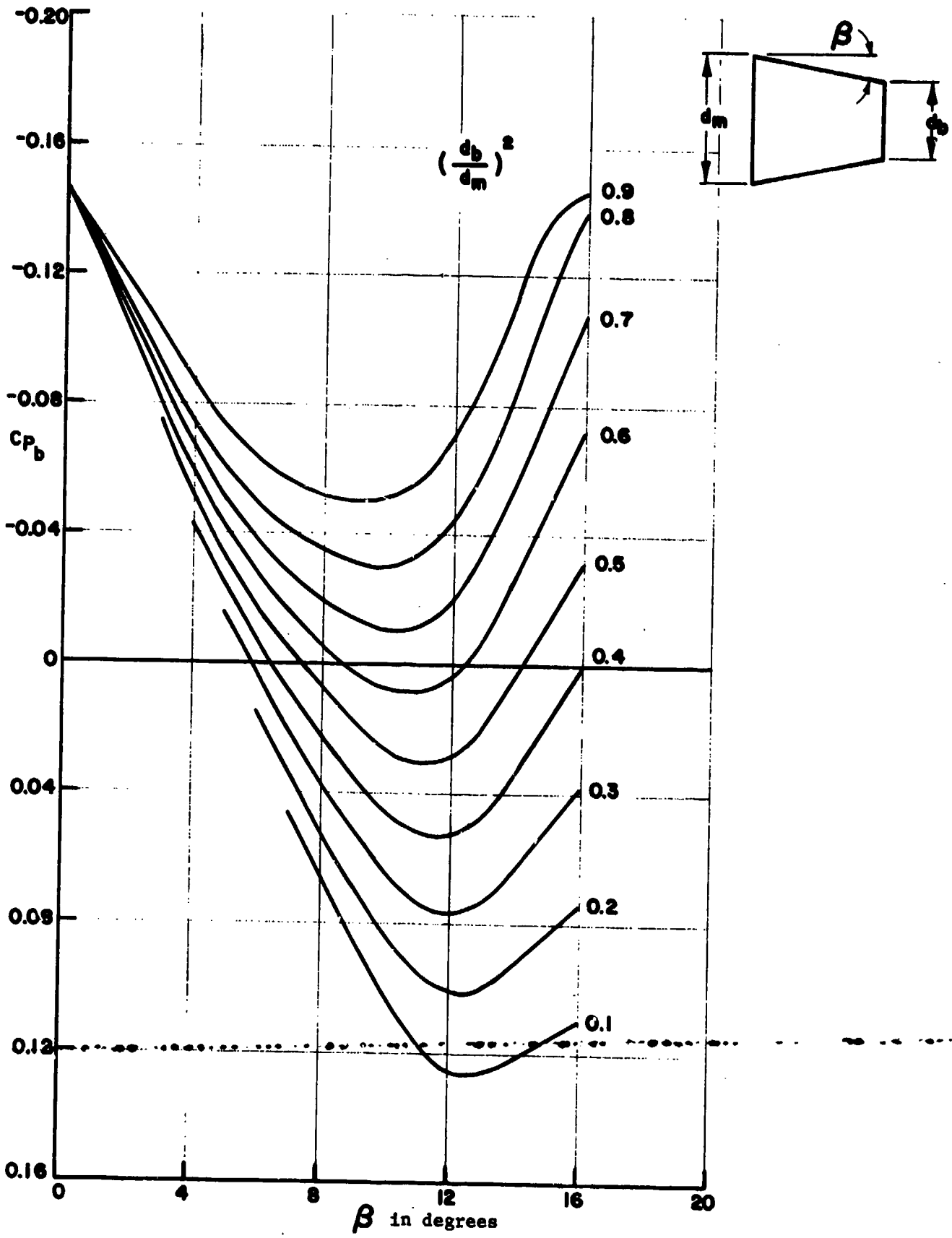

Figure 5c - M = 0.9

Figure 5 - Continued

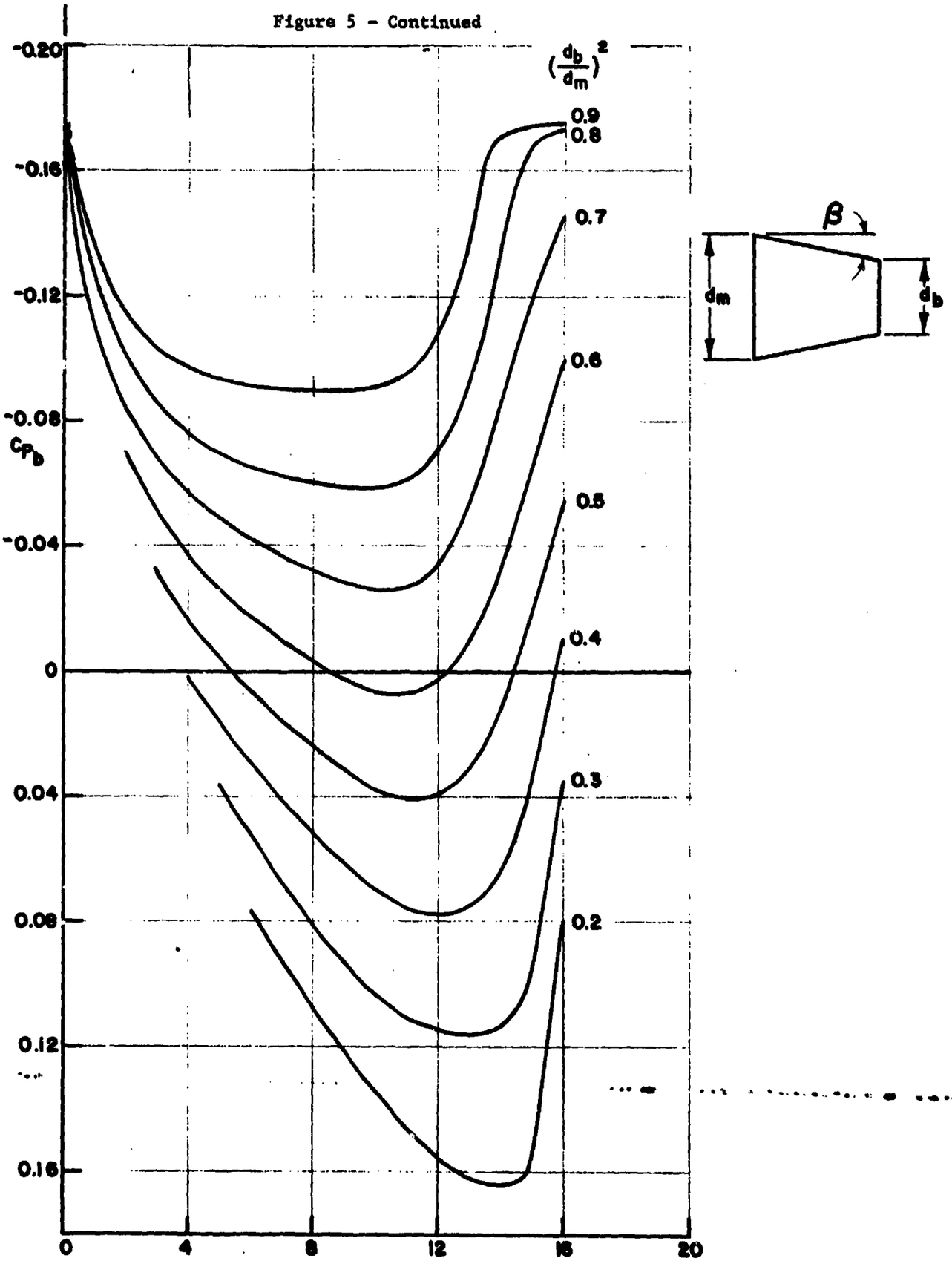

Figure 5d - M = 1.0

Figure 5 - Continued

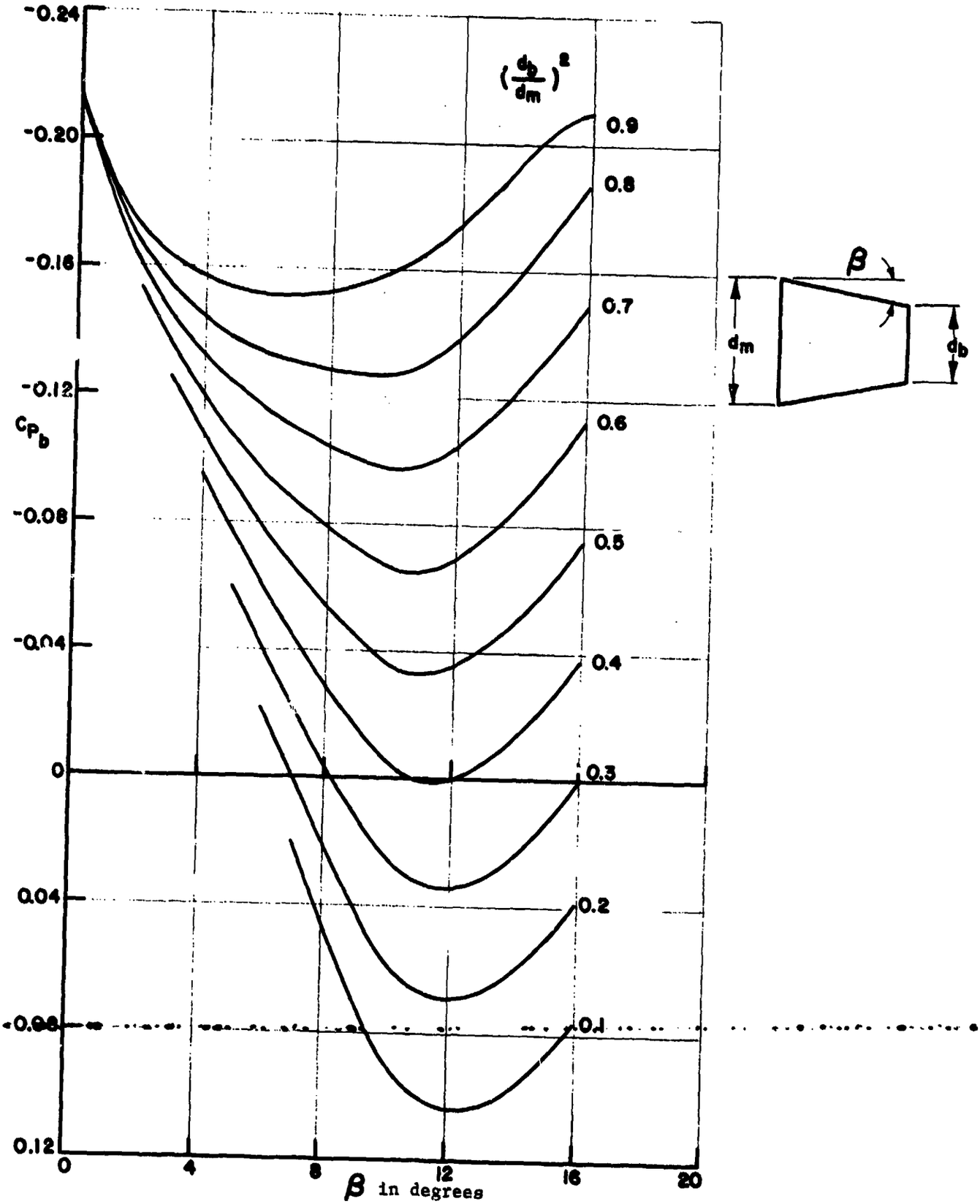

Figure 5e - M = 1.1

Figure 5 - Continued

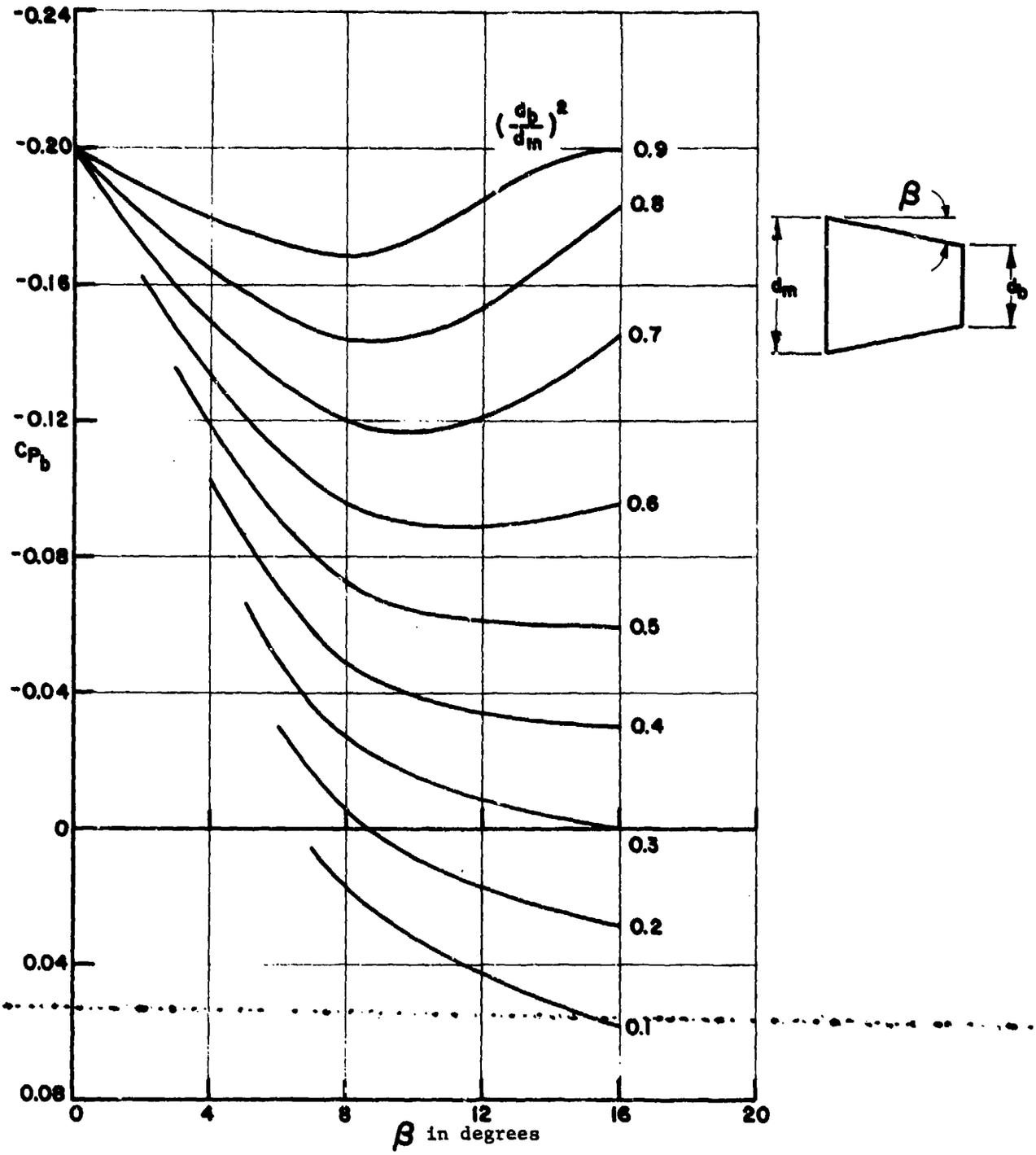

Figure 5f - M = 1.2

Figure 5 - Continued

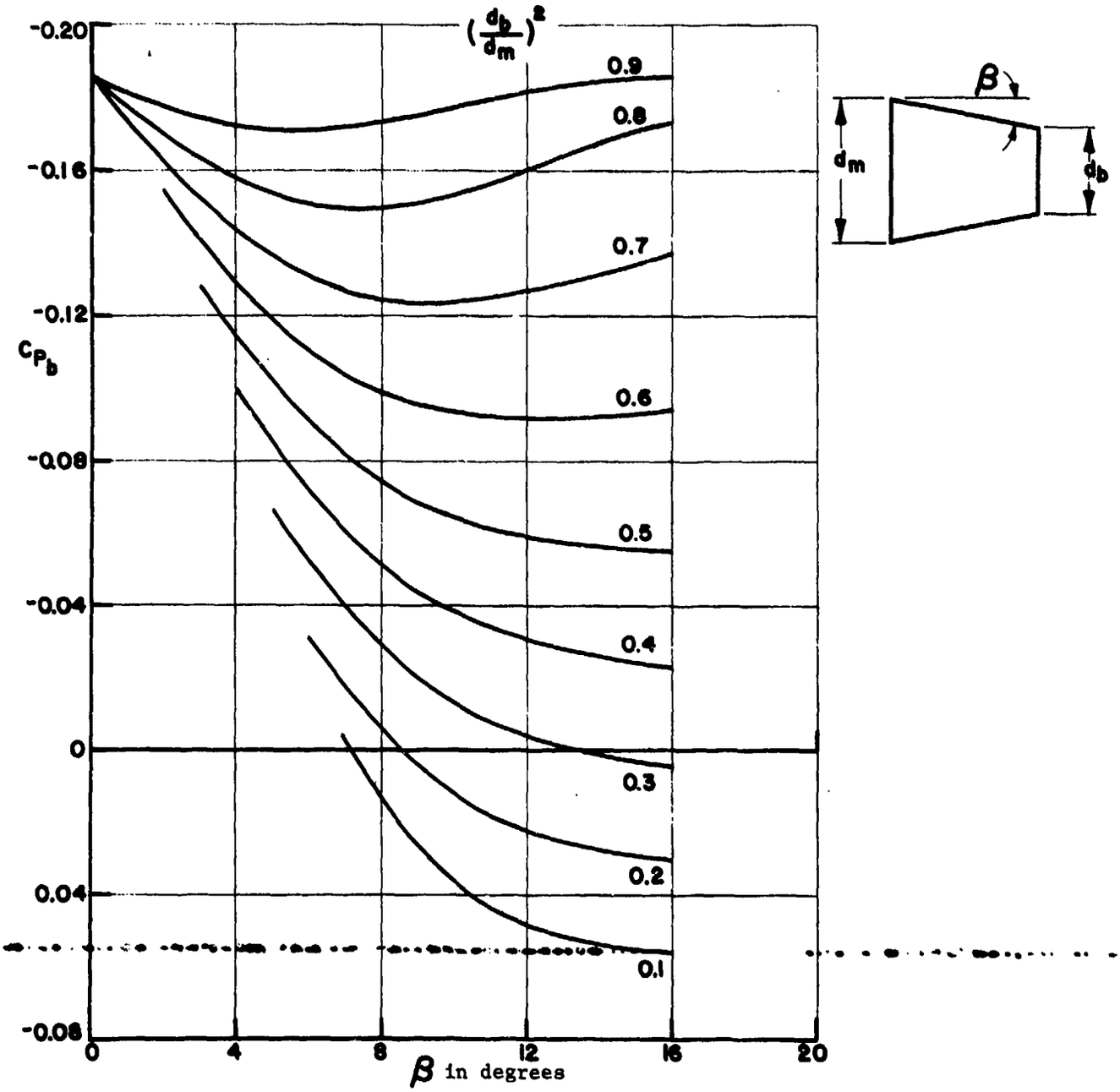

Figure 5g - M = 1.3

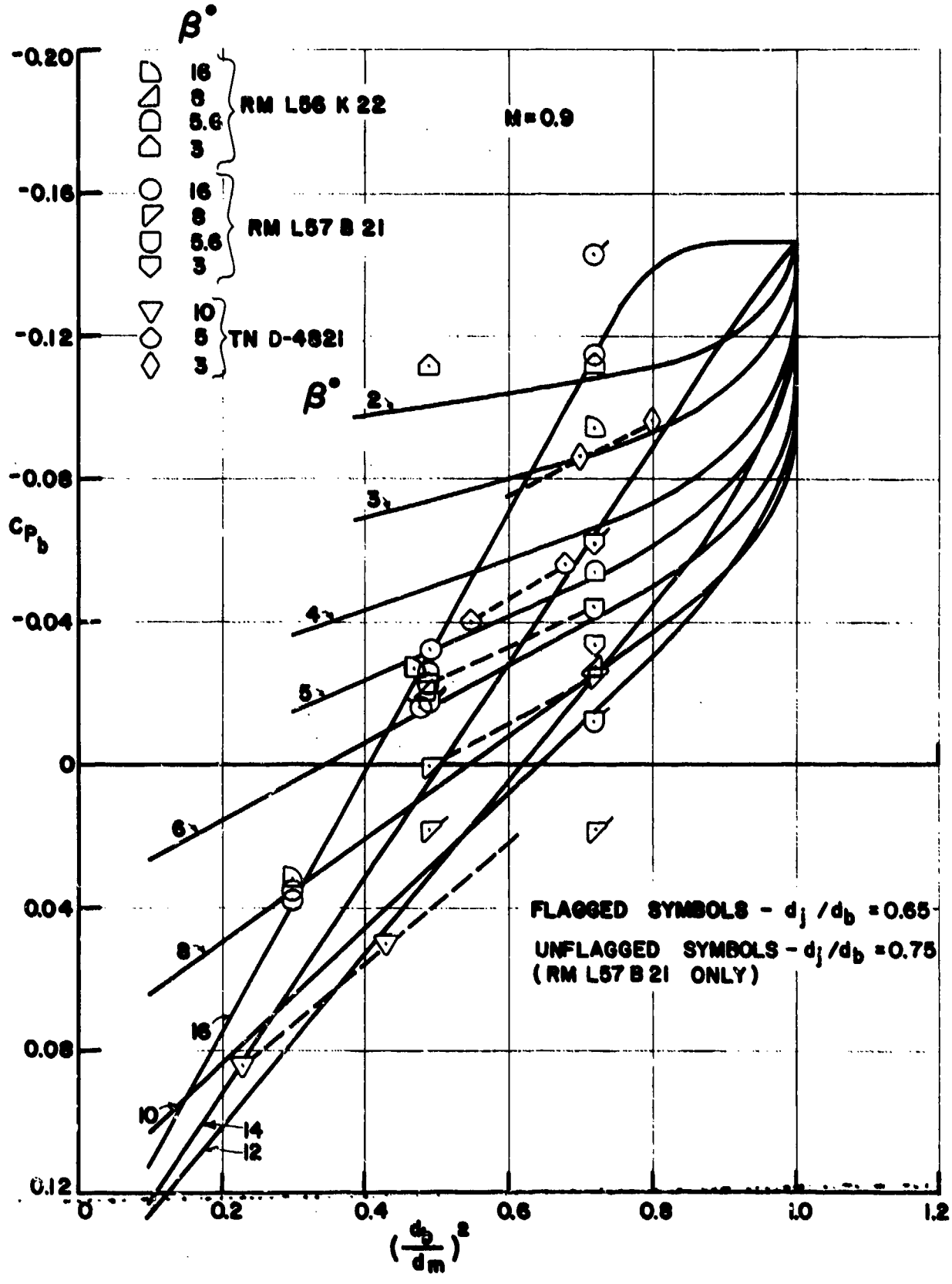

Figure 6 - A Correlation of Conical Boattail Base Pressure Coefficients as a Function of Base Diameter Ratio with Jet Off

RM L57 B 21
and
TN D-4821

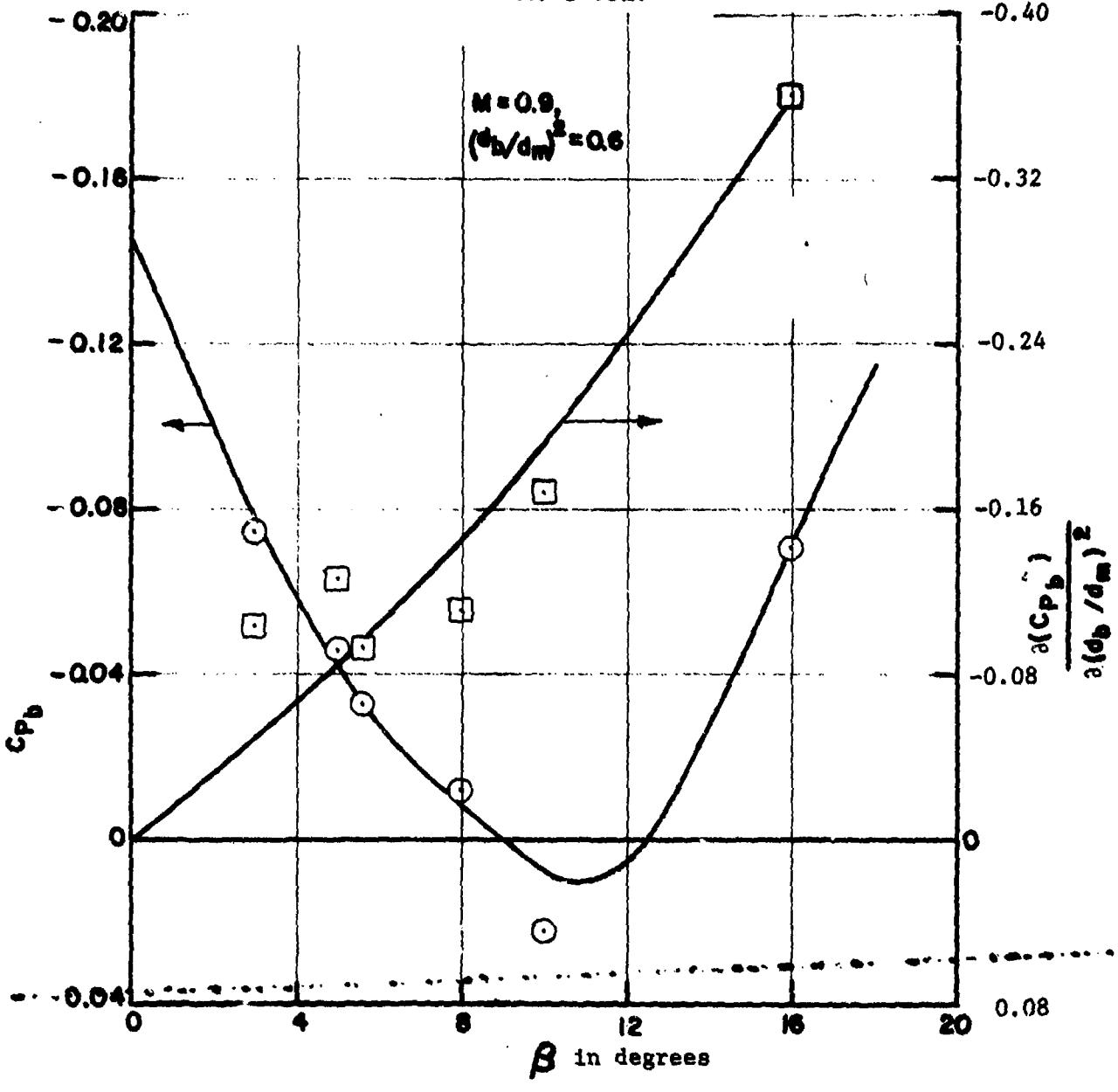

Figure 7 - A Correlation of Conical Boattail Base Pressure Coefficients as a Function of Boattail Angle with Jet Off

Figure 8 - Circular Arc Boattail Drag Coefficient with Jet Off

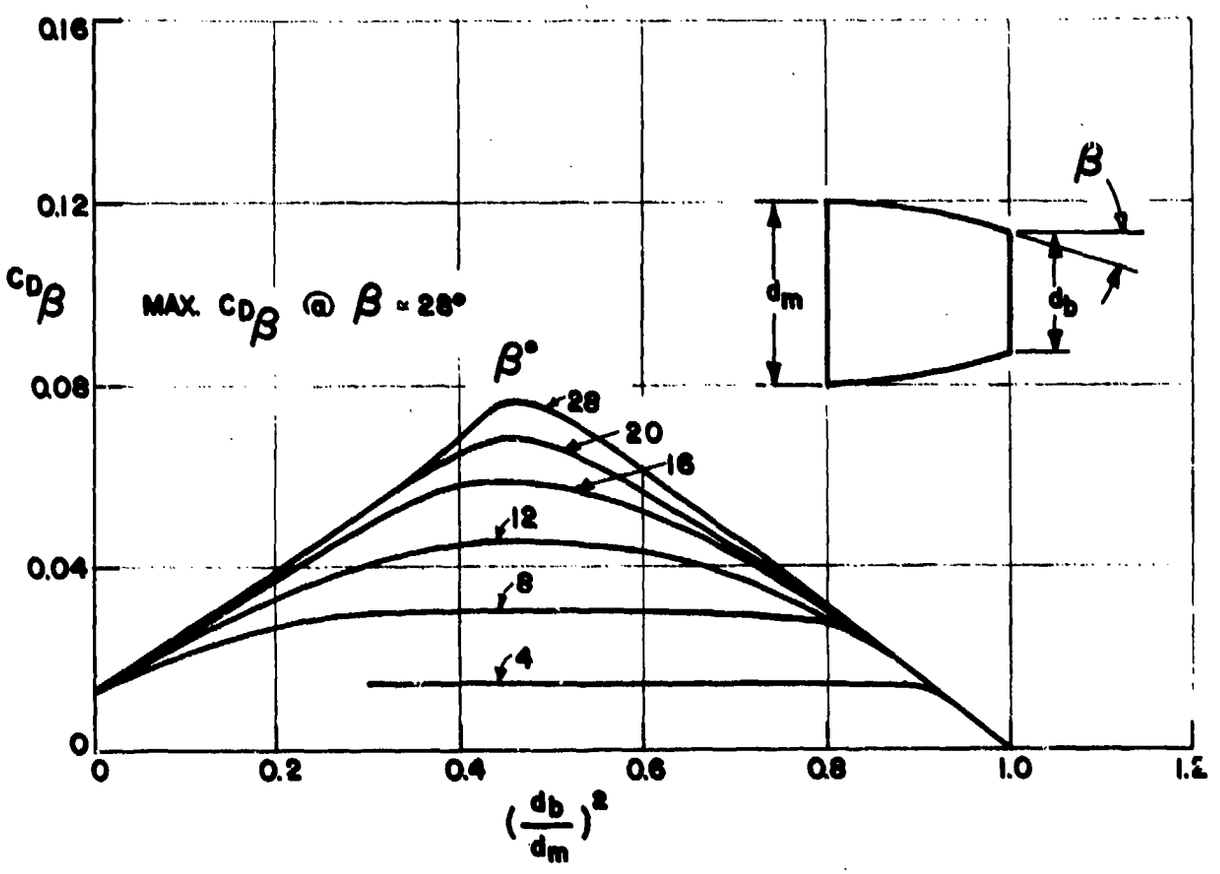

Figure 8a - M = 0.6

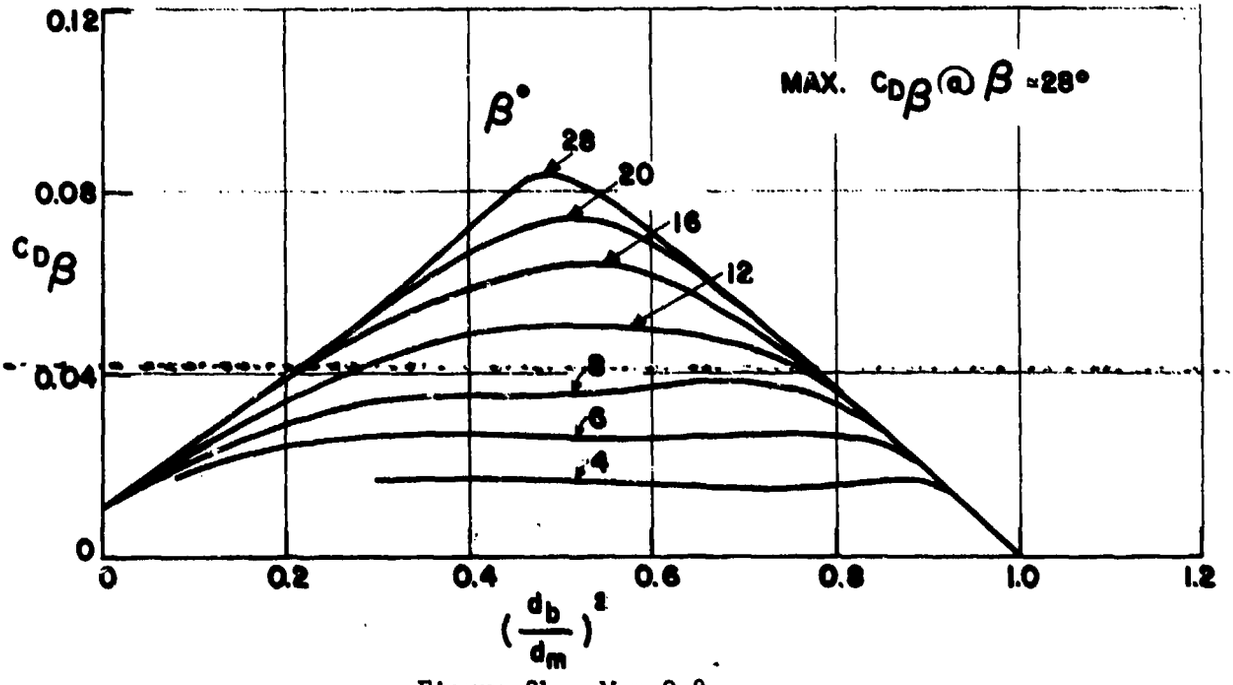

Figure 8b - M = 0.8

Figure 8 - Continued

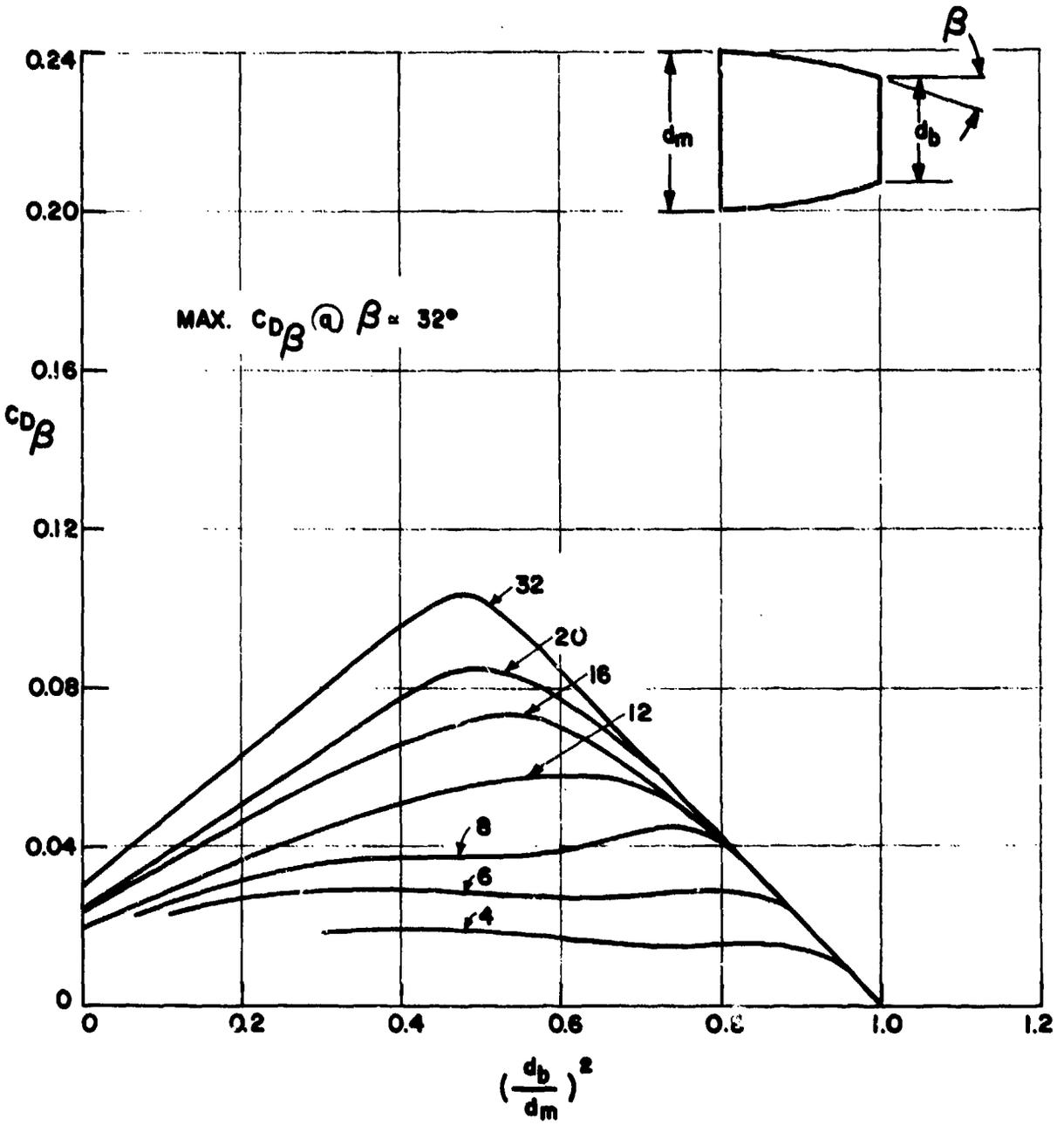

Figure 8c - M = 0.9

Figure 8 - Continued

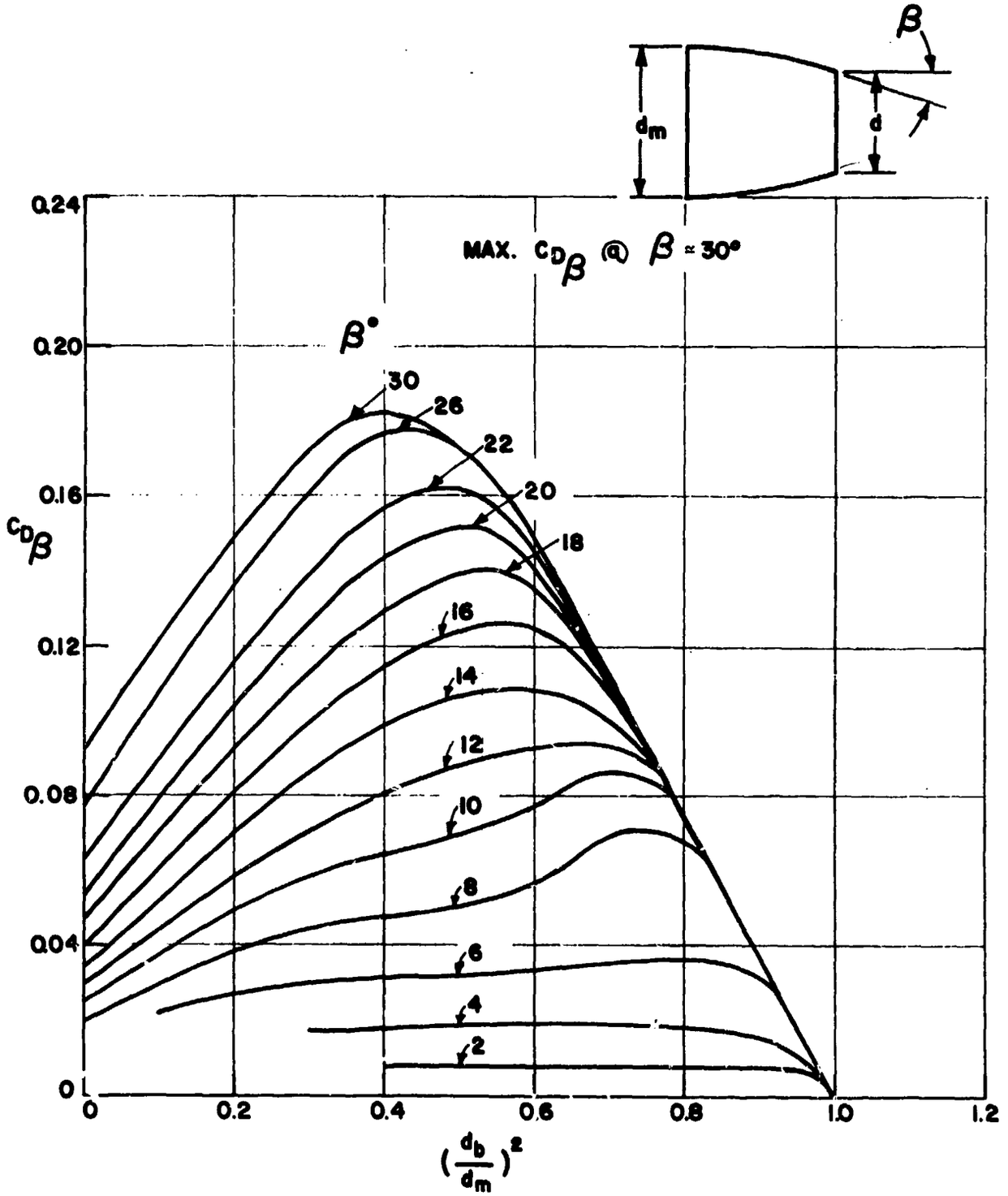

Figure 8d - M = 1.0

Figure 8 - Continued

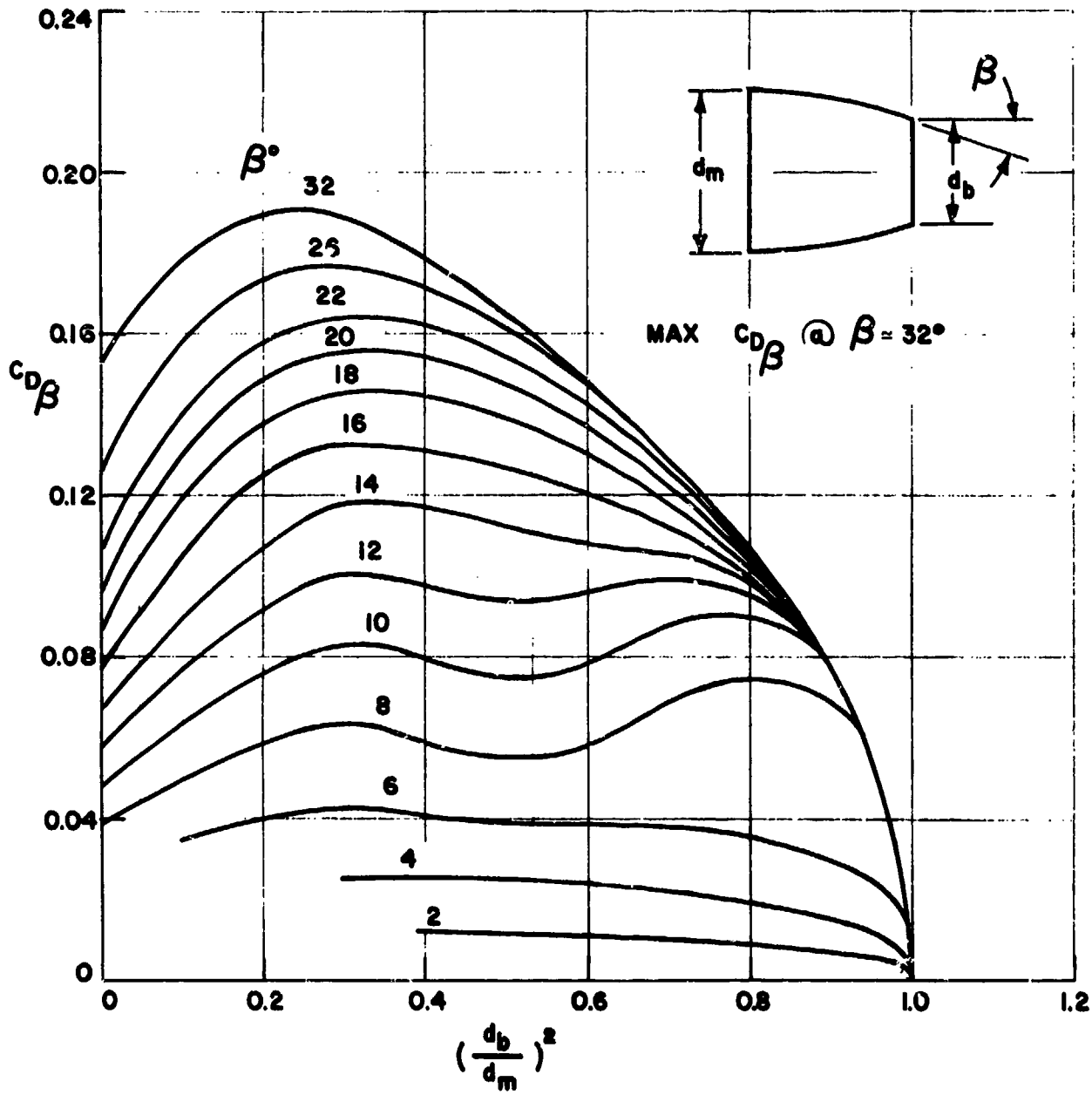

Figure 8e - M = 1.1

Figure 8 - Continued

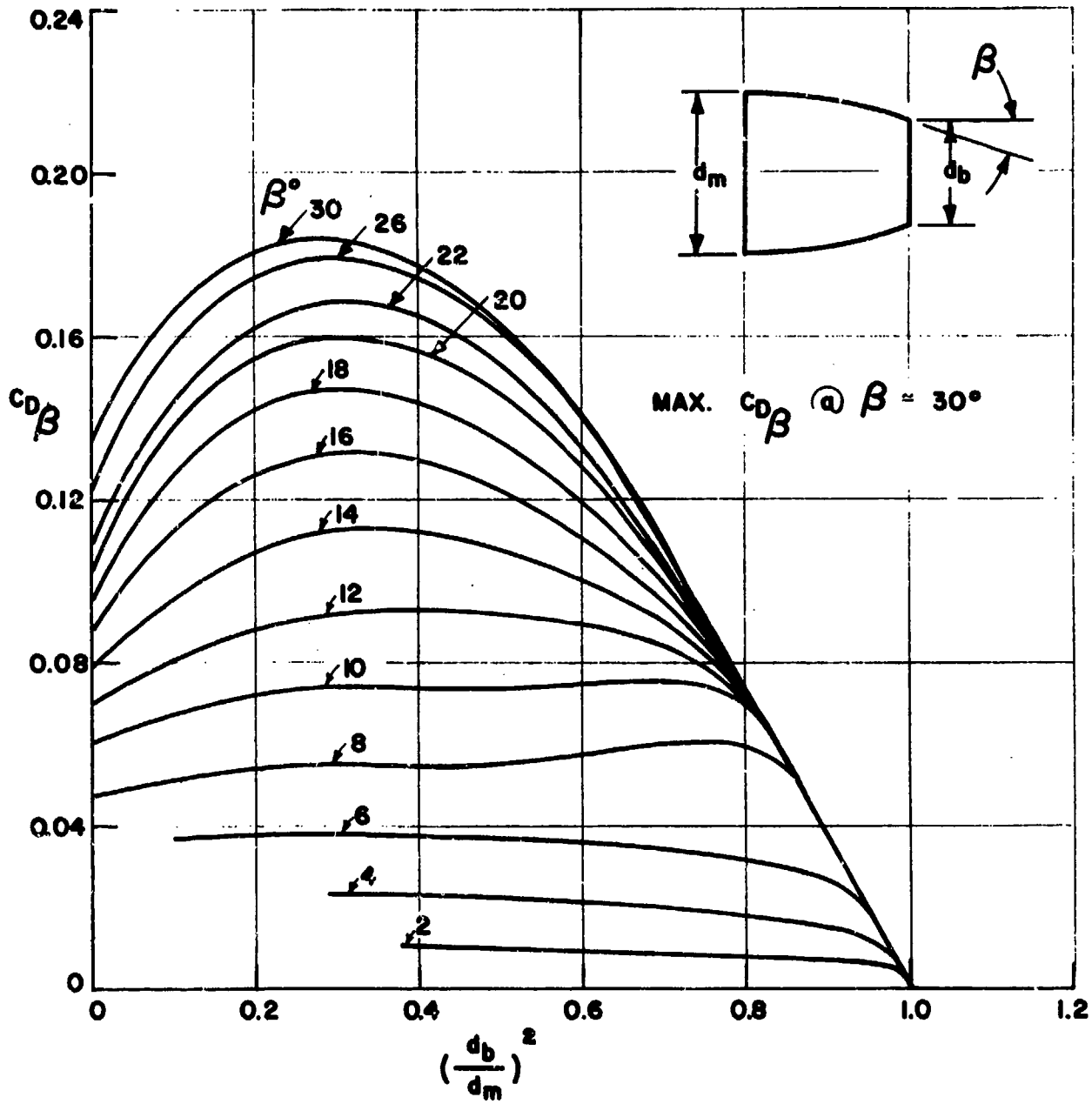

Figure 8 f - M = 1.2

Figure 8 - Continued

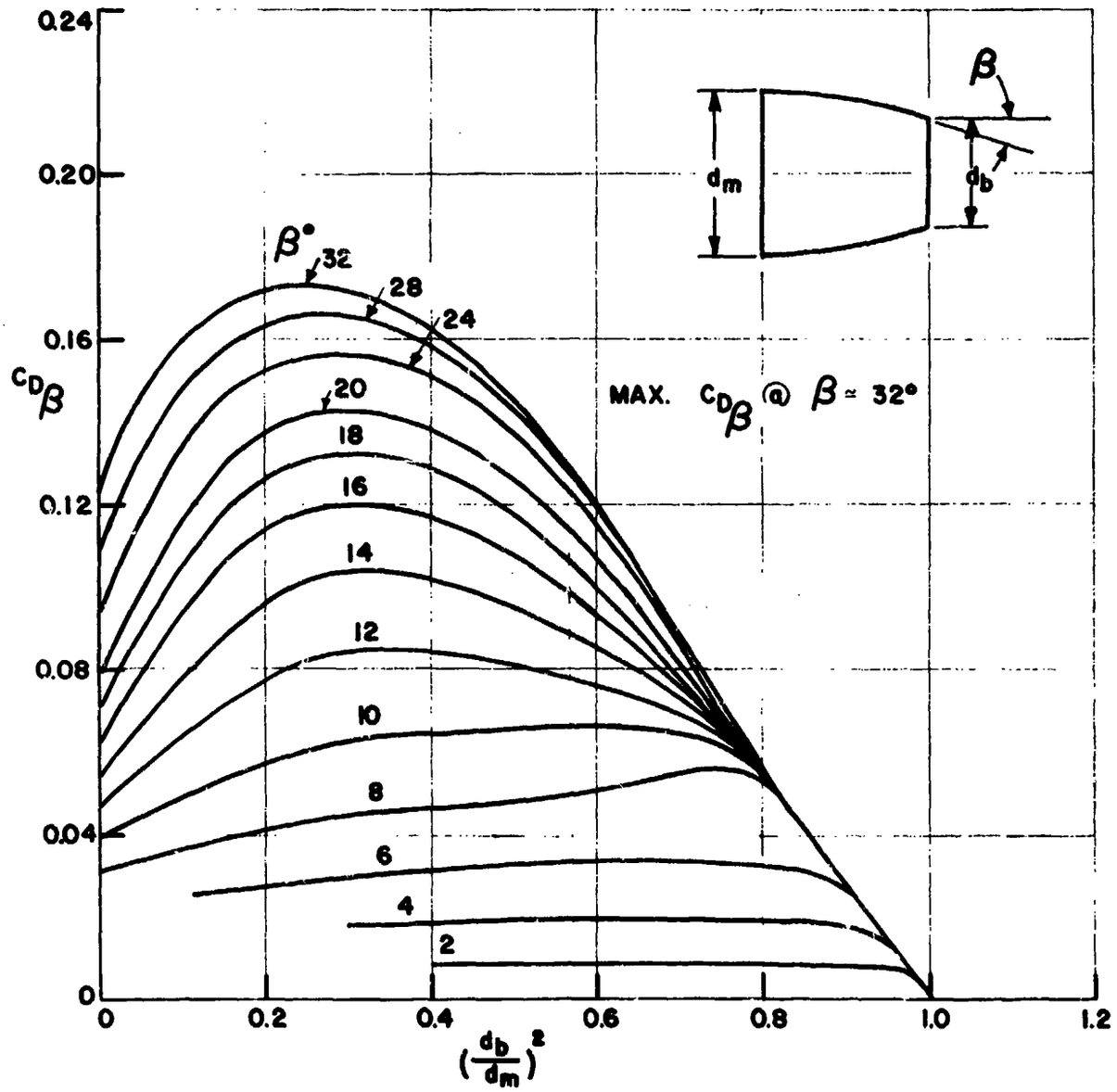

Figure 8g - M = 1.3

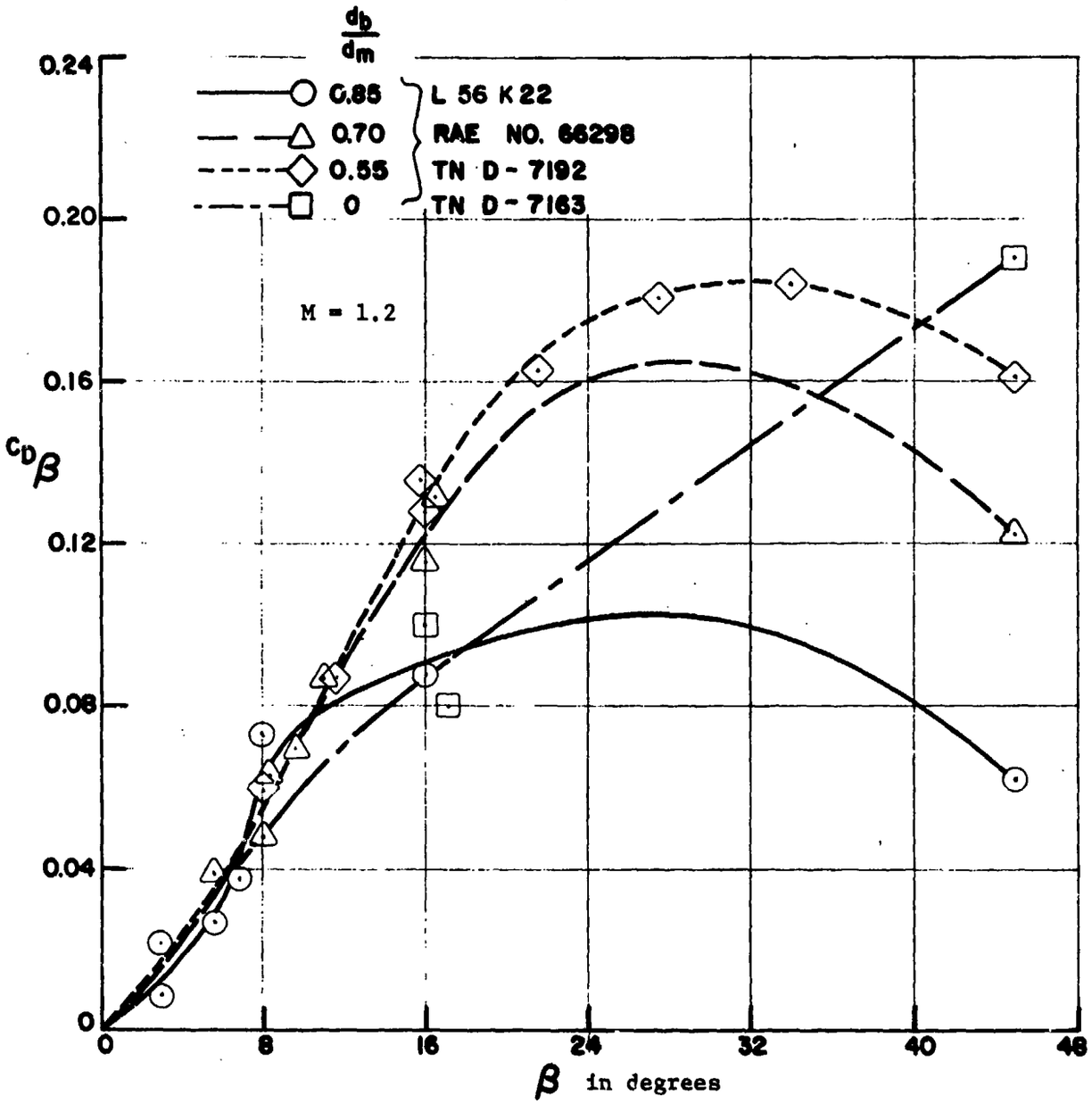

Figure 9 - A Correlation of Circular Arc Boattail Coefficients with Jet Off

Figure 10 - Circular Arc Boattail Base Pressure Coefficients with Jet Off

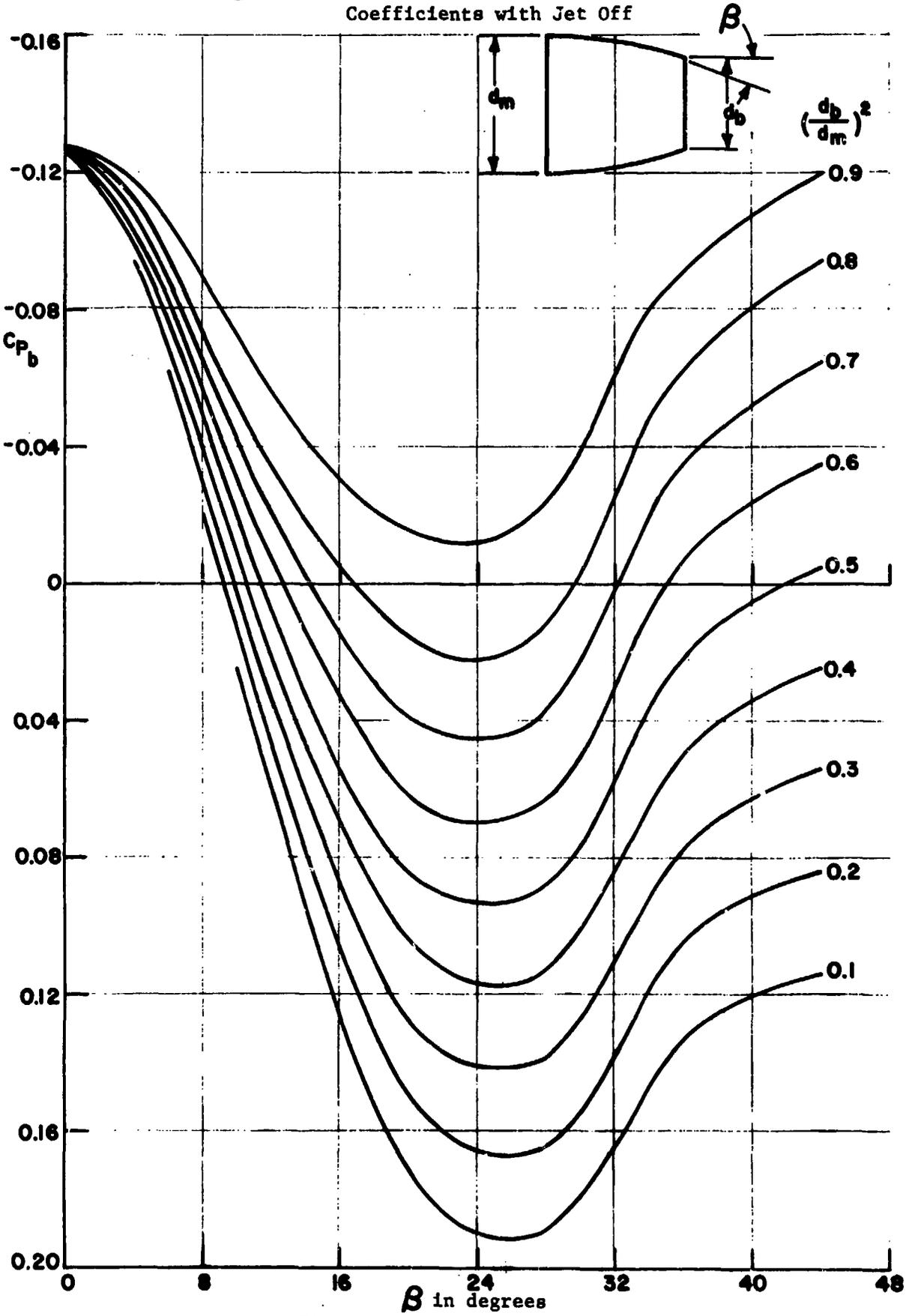

Figure 10a - M = 0.6

Figure 10 - Continued

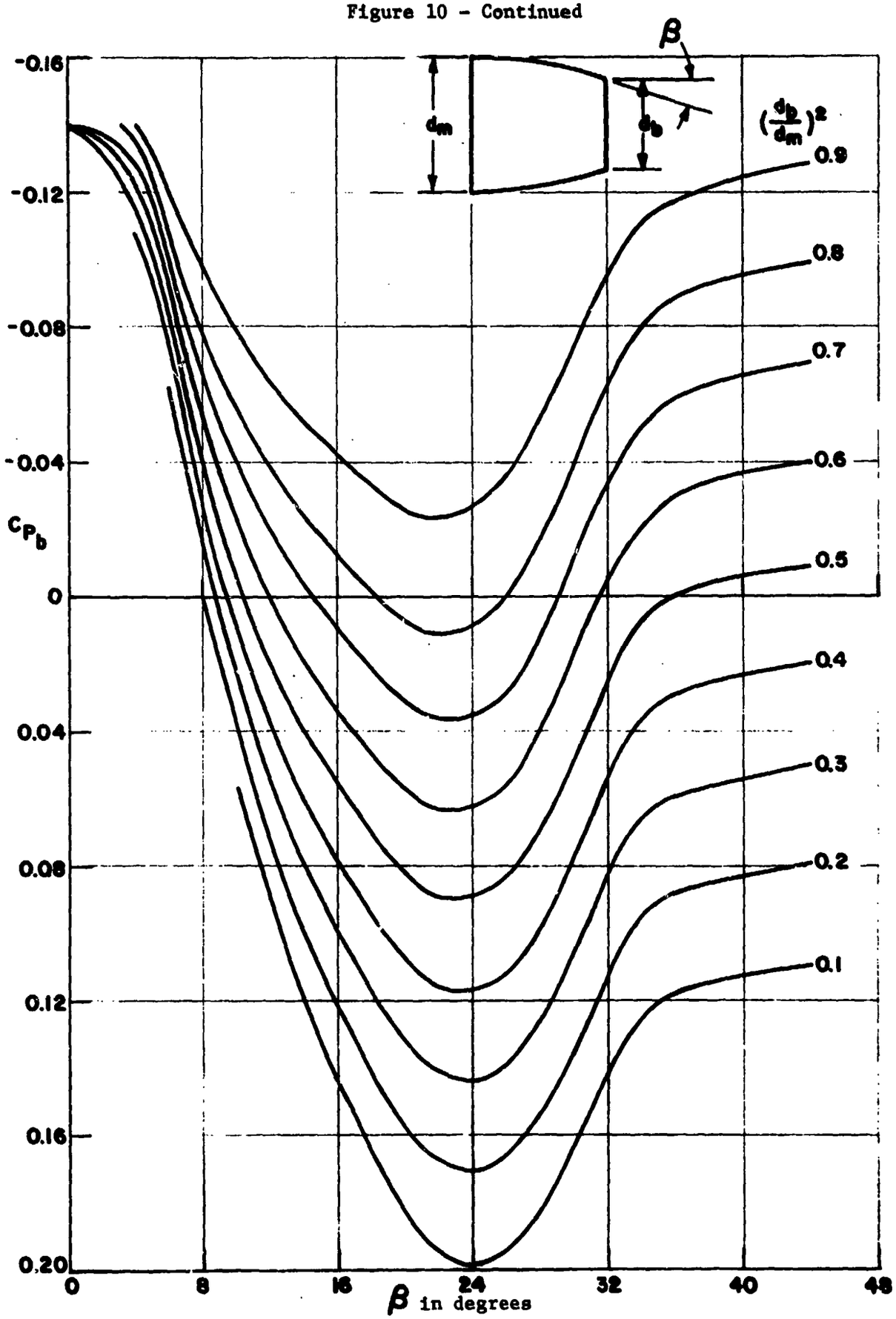

Figure 10b - M = 0.8

Figure 10 - Continued

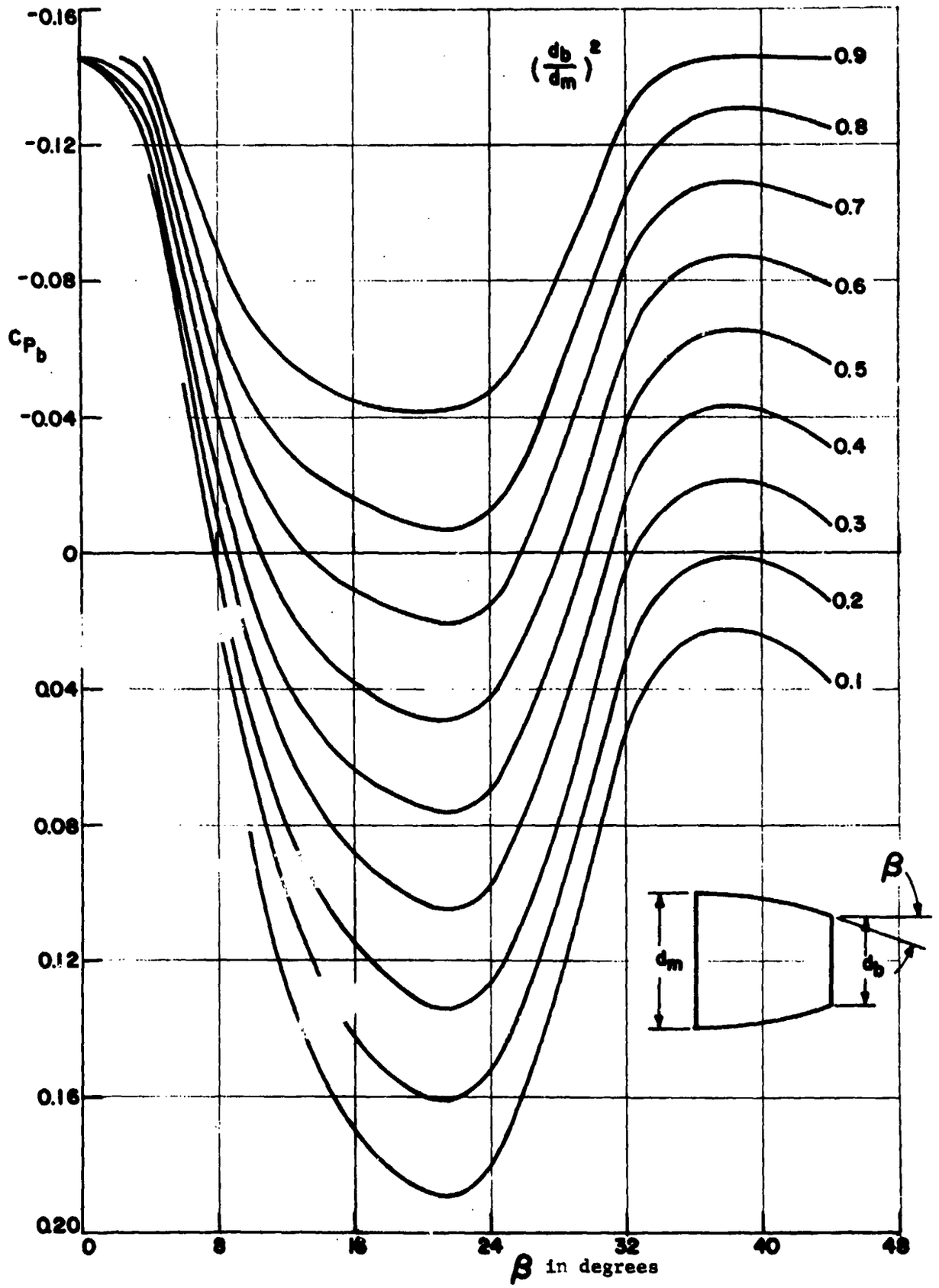

Figure 10c - M = 0.9

Figure 10 - Continued

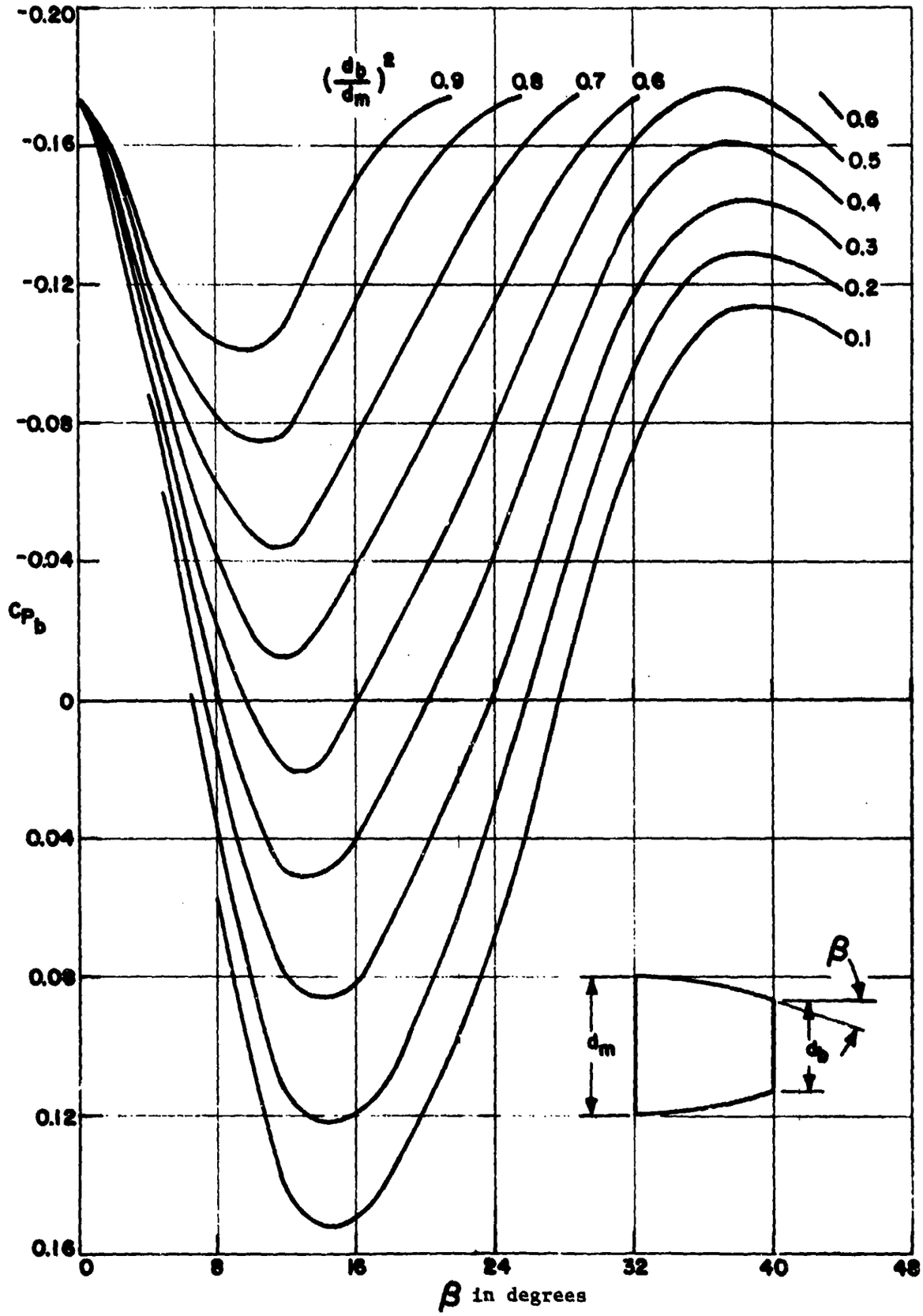

Figure 10d - M = 1.0

Figure 10 - Continued

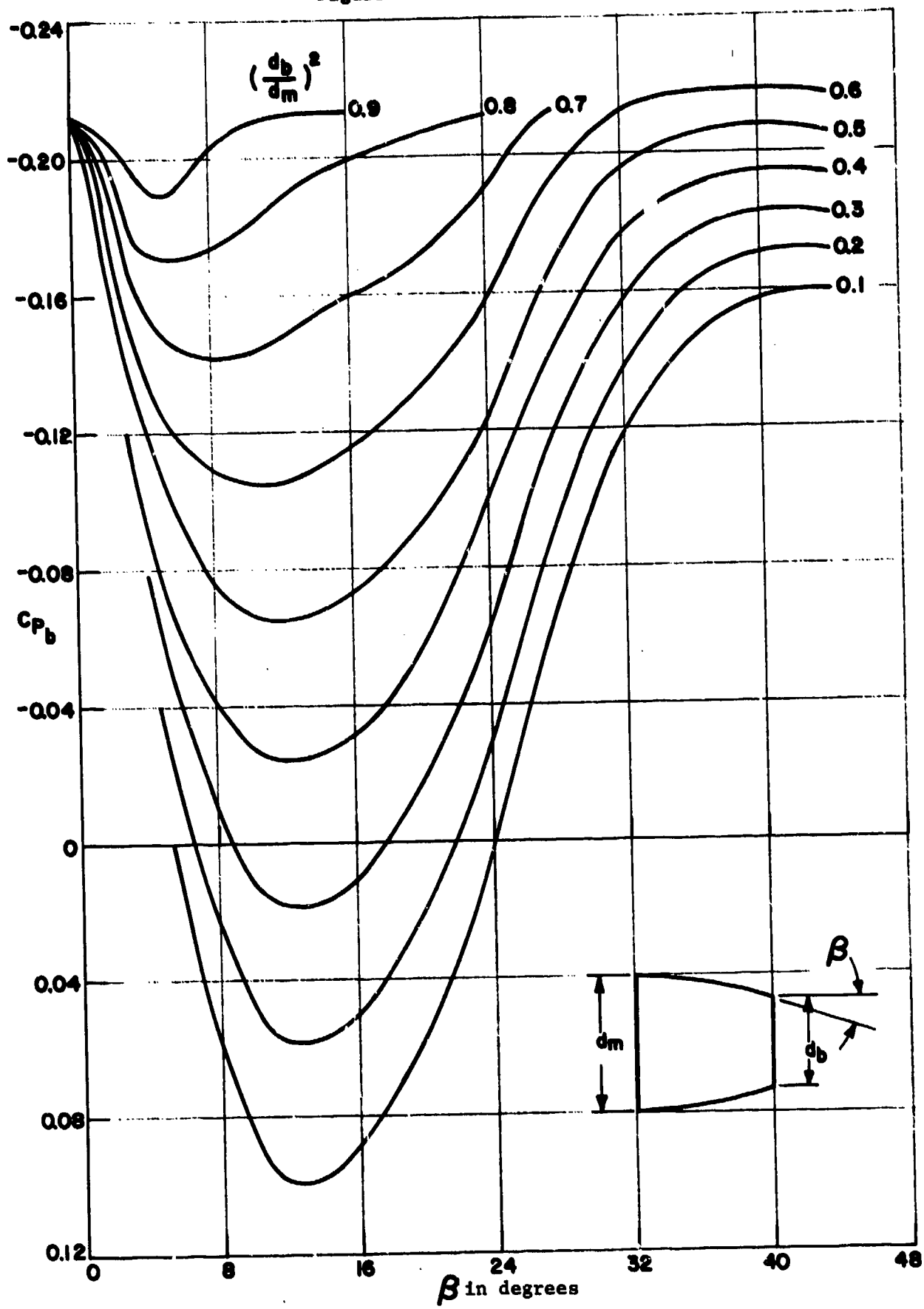

Figure 10e - M = 1.1

Figure 10 - Continued

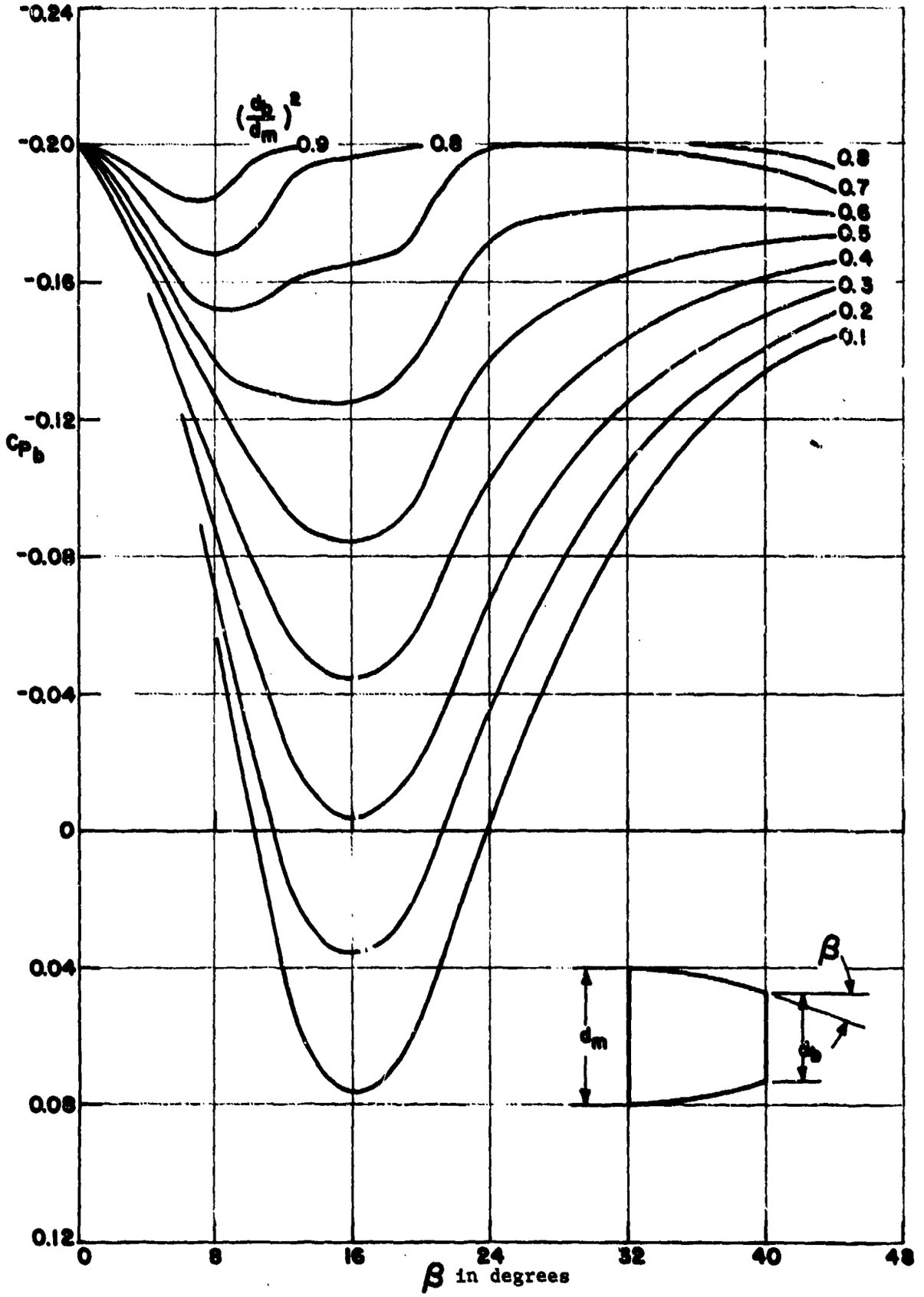

Figure 10f - M = 1.2

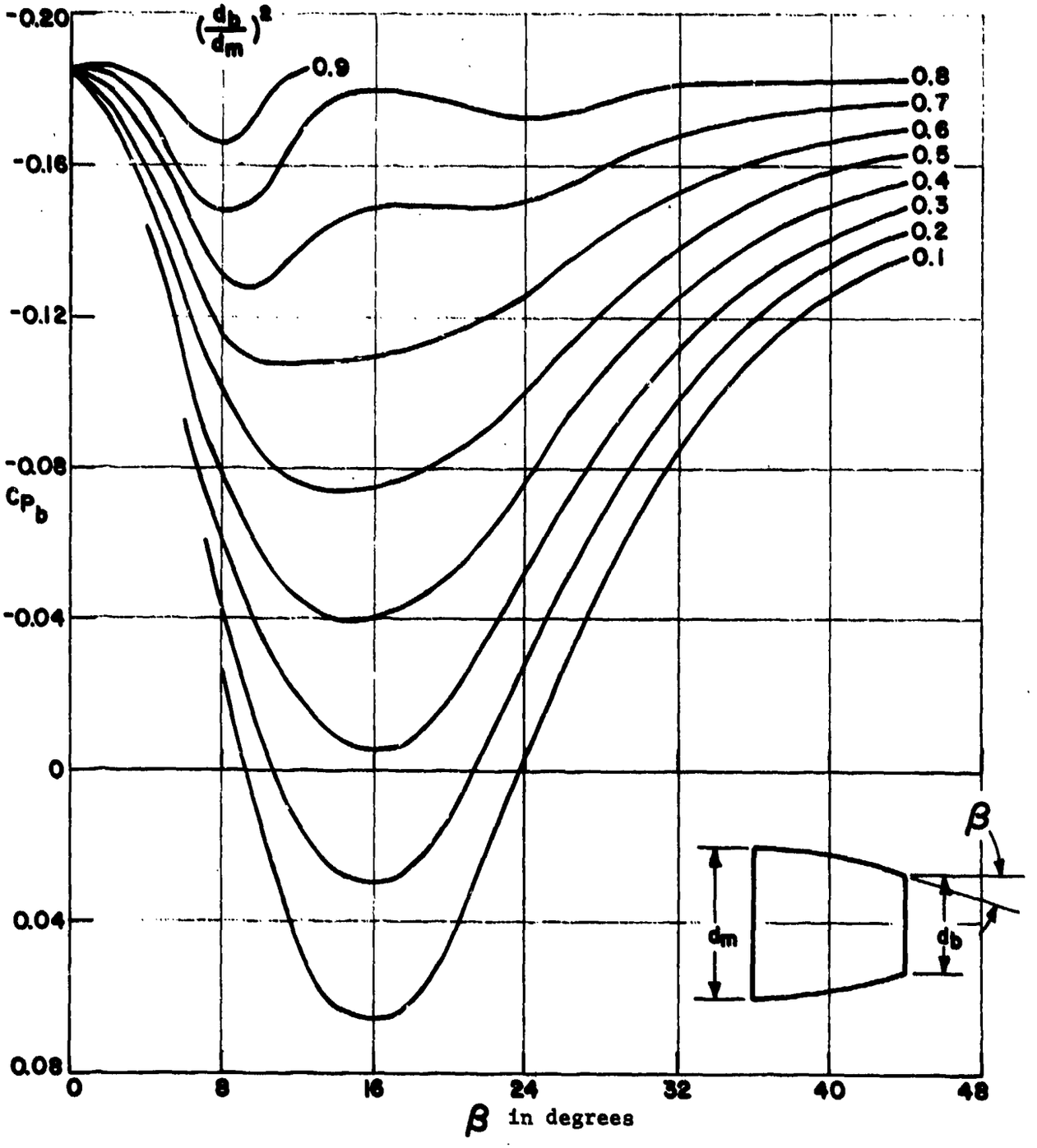

Figure 10g - M = 1.3

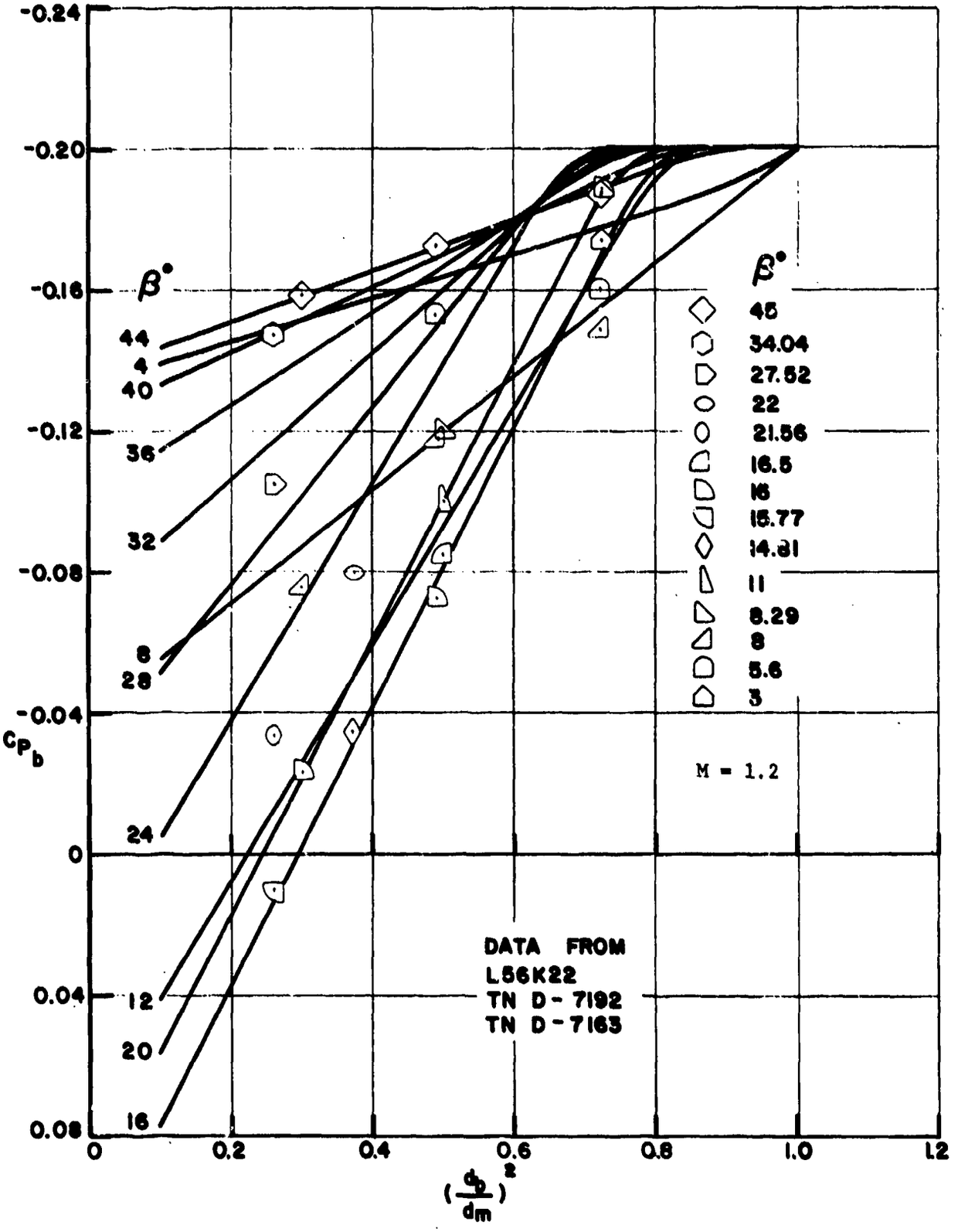

Figure 11 - A Correlation of Circular Arc Boattail Base Pressure Coefficients as a Function of Base Diameter Ratio with Jet Off

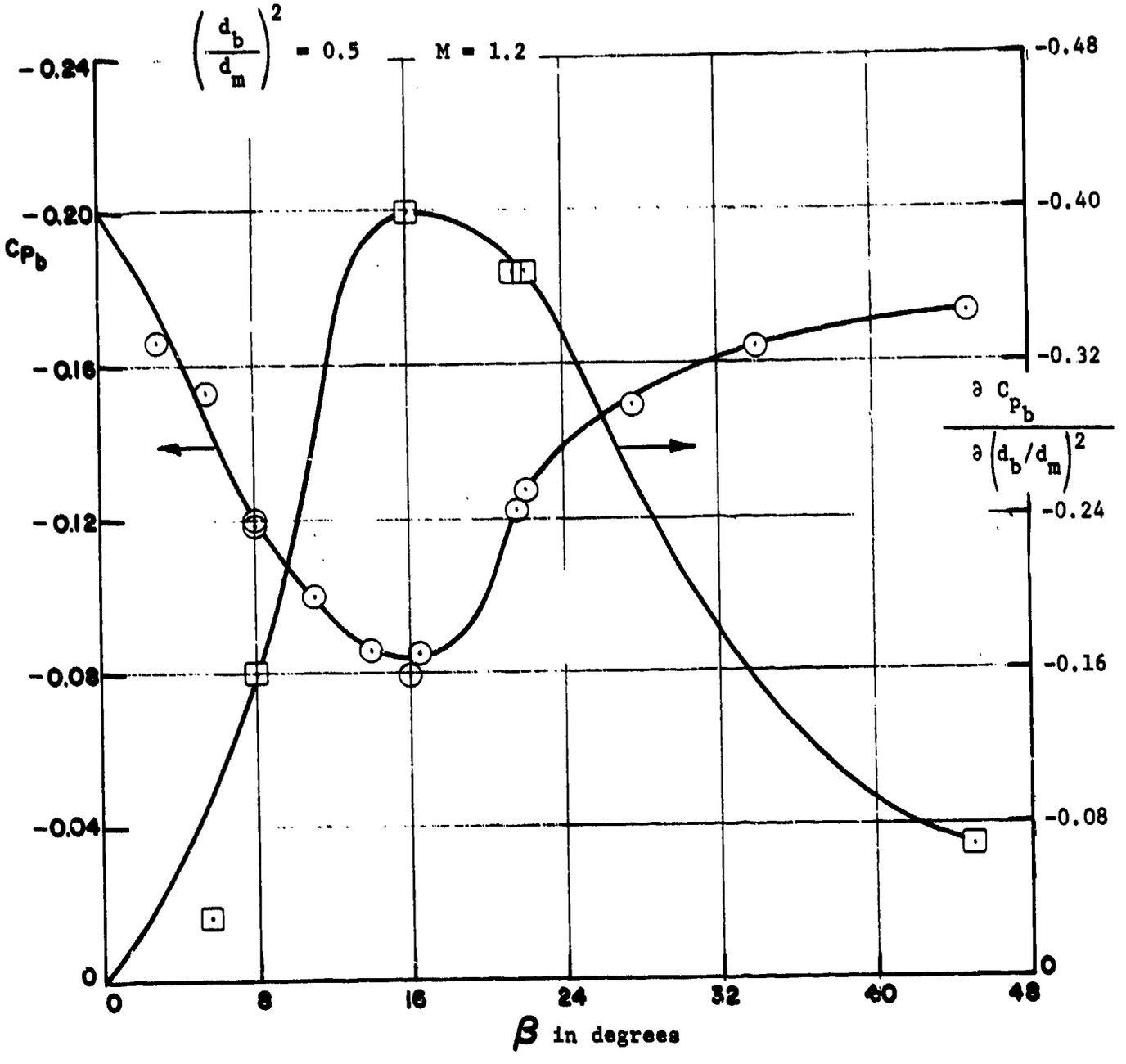

Figure 12 - A Correlation of Circular Arc Boattail Base Pressure Coefficients as a Function of Boattail Angle with Jet Off

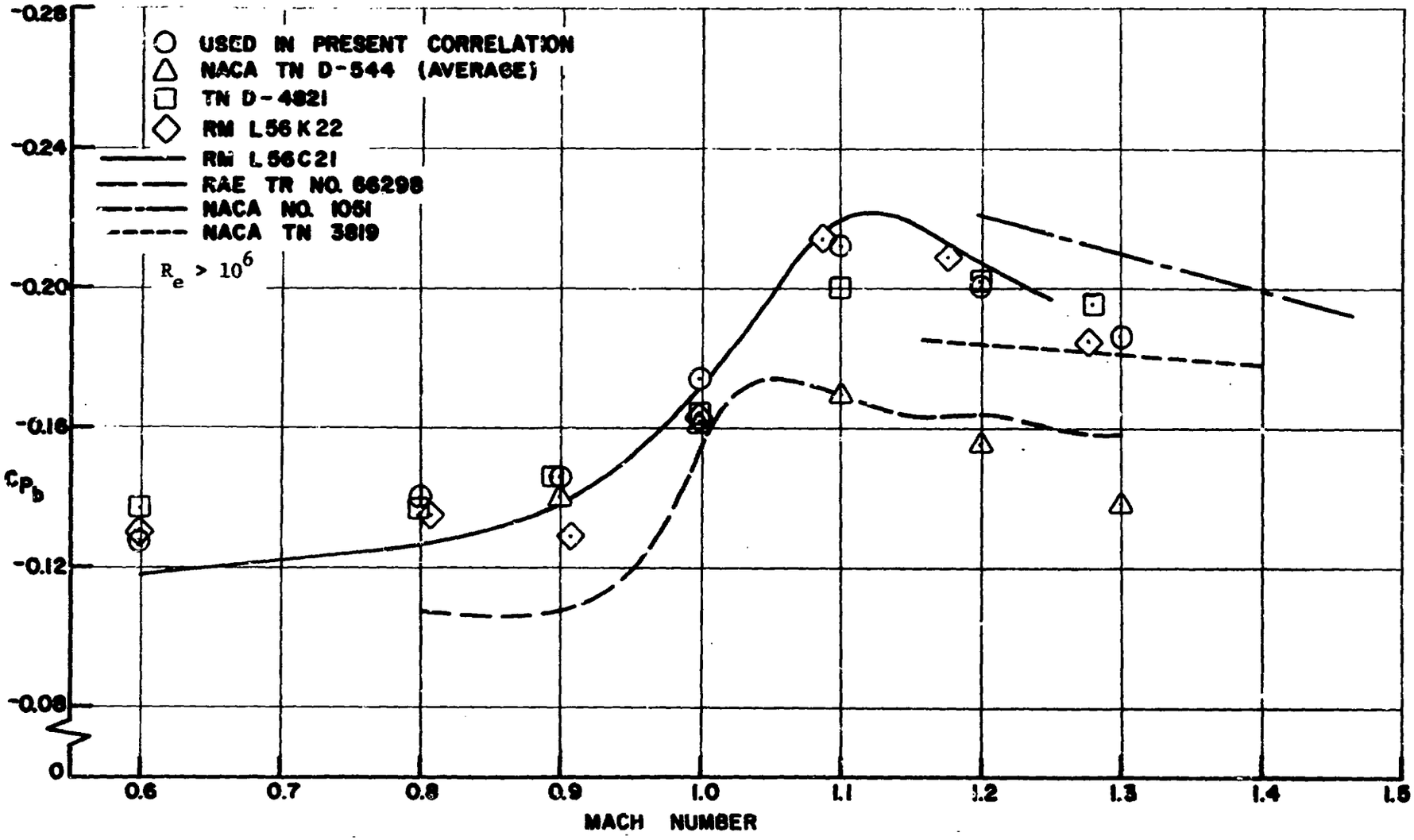

Figure 13 - Cylindrical Afterbody Base Pressure Coefficients with Turbulent Boundary Layer

REFERENCES

1. Cubbage, J.M., Jr., "Jet Effects on the Drag of Conical Afterbodies for Mach Numbers of 0.6 to 1.28," NACA RM L57B21 (Apr 1957).

2. Silhan, F.F. and J.M. Cubbage, Jr., "Drag of Conical and Circular Arc Boattailed Afterbodies at Mach 0.6 to 1.3," NACA RM L56K22 (Jan 1957).

3. Compton, W.B., III, "Effect on Base Drag of Recessing the Bases of Conical Afterbodies at Subsonic and Transonic Speeds," NASA TN D-4821 (Oct 1968).

4. Cubbage, J.M., Jr., "Jet Effects on Base and Afterbody Pressures of a Cylindrical Afterbody at Transonic Speeds," NACA RM L56C21 (May 1956).

5. Cubbage, J.M., Jr. and E.H. Andrews, Jr., "Measured Base Pressures on Several Twin Rocket-Nozzle Configurations at Mach Numbers of 0.5 to 1.4 with Effects Due to Nozzle Canting and Stabilizing Fins," NASA TN D-544 (Nov 1960).

6. Compton, W.B., III, "Jet Effects on the Drag of Conical Afterbodies at Supersonic Speeds," NASA TN D-6789 (Jul 1972).

7. Compton, W.B., III and J.F. Runckel, "Jet Effects on the Boattail Force Coefficient of Conical Afterbodies at Subsonic and Transonic Speeds," NASA TM X-1960 (Feb 1970).

8. Kurn, A.G., "Drag Measurements on a Series of Afterbodies at Transonic Speeds Showing the Effect of Sting Interference," Royal Aircraft Establishment, Technical Report No. 66298 (Sep 1966).

9. Reubush, D.E., "Effects of Fineness and Closure Ratios on Boattail Drag of Circular-Arc Afterbody Models with Jet Exhaust at Mach Numbers up to 1.3," NASA TN D-7163 (May 1973).

10. Reubush, E.E. and J.F. Runckel, "Effect of Fineness Ratio on the Boattail Drag of Circular-Arc Afterbodies Having Closure Ratios of 0.50 with Jet Exhaust at Mach Numbers up to 1.30," NASA TN D-7192 (May 1973).

11. McDonald, H. and P.F. Hughes, "A Correlation of High Subsonic Afterbody Drag in the Presence of a Propulsive Jet or Support Sting," J. of Aircraft, Vol. 2, No. 3 (May-Jun 1965).

12. Bergman, D., "An Aerodynamic Drag Study of Jet Engine Nozzles," AGARD Paper 22, CP-91-71 (Sep 1971).

13. Bergman, D., "An Afterbody Drag Approximation Procedure Based on Empirical Correlations," Propulsion Interaction Workshop, NASA Langley Research Center, p. 273-489 (May 1976).

14. Swavely, C.E. and J.F. Soileau, "Aircraft Afterbody/Propulsion System Intergration for Low Drag," AIAA Paper No. 72-1101 presented at the AIAA/SAE 8th Joint Propulsion Specialist Conference, New Orleans, Louisiana (29 Nov - 1 Dec 1972).

15. Brazier, M. and W.H. Ball, "Accounting of Aerodynamic Forces on Airframe/Propulsion Systems," Paper No. 22 in AGARD CP-150, Fluid Dynamics Panel Symposium (Sep 1974).

16. Presz, W.M., Jr. and E.T. Pitkin, "Analytical Model of Axisymmetric Afterbody Flow Separation," J. of Aircraft, Vol. 13, No. 7 (Jul 1976).

17. Chapman, D.R., "An Analysis of Base Pressure at Supersonic Velocities and Comparison with Experiment," NACA Report No. 1051 (1950).

18. Love, E.S., "Base Pressure at Supersonic Speeds on Two-Dimensional Airfoils and Bodies of Revolution With and Without Fins Having Turbulent Boundary-Layers," NACA TN 3819 (1957).

19. Brazzel, C.E. and Y.H. Henderson, "An Empirical Technique for Estimating Power-On Base Drag of Bodies-of-Revolution with Single Jet Exhaust," USAMC, Redstone Arsenal, AGARD Conference Proceedings #10 (Sep 1966).

20. Addy, A.L., "Analysis of the Axisymmetric Base Pressure and Base Temperature Problem with Supersonic Interacting Freestream-Nozzle Flows Based on the Flow Model of Korst, et al., Part I: A Computer Program and Representative Results for Cylindrical Afterbodies," USAMC, Redstone Arsenal, Alabama, RD-TR-69-12 (Jul 1969).

21. Addy, A.L., "Analysis of the Axisymmetric Base Pressure and Base Temperature Problem with Supersonic Interacting Freestream-Nozzle Flows Based on the Flow Model of Korst, et al., Part II: A Comparison and Correlation with Experiment for Cylindrical Afterbodies," USAMC, Redstone Arsenal, Alabama, RD-TR-69-13 (Dec 1969).

22. Addy, A.L., "Analysis of the Axisymmetric Base Pressure and Base Temperature Problem with Supersonic Interacting Freestream-Nozzle Flows Based on the Flow Model of Korst, et al., Part III: A Computer Program and Representative Results for Cylindrical, Boattailed or Flared Afterbodies," USAMC, Redstone Arsenal, RD-TR-69-14 (Feb 1970).

23. King, M.A., "An Assessment of a Method Developed by U.S. Army Missile Command for Predicting Base Pressure of a Body of Revolution with a Hot Jet Efflux," British Aircraft Corp. Limited, Guided Weapons Division, Bristol, Report ST 14691 (Mar 1976).

24. Reid, J. and R.C. Hastings, "Experiments on the Axisymmetric Flow Over Afterbodies and Bases at M = 2.0," Royal Aircraft Establishment (Farnborough), Report No. AERO. 2628 (Oct 1959).

25. Boren, T.C. and D.E. Stevens, "Afterbody Drag Study," Convair/Pomona, Convair Division of General Dynamics Corp., Technical Memorandum TM No. 334-456 (Jan 1961).

26. Shrewsbury, G.D., "Effect of Boattail Juncture Shape on Pressure Drag Coefficients of Isolated Afterbodies," NASA TM X-1517 (Mar 1968).

27. Wilcox, F.A. and R. Chamberlin, "Reynolds Number Effects on Boattail Drag of Exhaust Nozzles from Wind Tunnel and Flight Tests," NASA TM X-71548 (Sep 1974).

28. Reubush, D.E., "The Effect of Reynolds Number on Boattail Drag," AIAA Paper No. 75-63, AIAA 13th Aerospace Sciences Meeting (20-22 Jan 1975).

29. Dansby, T., "Reynolds Number Effects on the Boattail Characteristics of a Simulated Nacelle at a Mach Number of 0.8," Aerospace Research Laboratories, Wright-Patterson Air Force Base, ARL TR 74-0120 (Oct 1974).

30. Aulehla, F. and G. Besigk, "Reynolds Number Effects on Fore- and Afterbody Pressure Drag," AGARD Conference Proceedings No. 150, Paper No. 12 (Sep 1974).

DTNSRDC ISSUES THREE TYPES OF REPORTS

1. DTNSRDC REPORTS, A FORMAL SERIES, CONTAIN INFORMATION OF PERMANENT TECHNICAL VALUE. THEY CARRY A CONSECUTIVE NUMERICAL IDENTIFICATION REGARDLESS OF THEIR CLASSIFICATION OR THE ORIGINATING DEPARTMENT.

2. DEPARTMENTAL REPORTS, A SEMIFORMAL SERIES, CONTAIN INFORMATION OF A PRELIMINARY, TEMPORARY, OR PROPRIETARY NATURE OR OF LIMITED INTEREST OR SIGNIFICANCE. THEY CARRY A DEPARTMENTAL ALPHANUMERICAL IDENTIFICATION.

3. TECHNICAL MEMORANDA, AN INFORMAL SERIES, CONTAIN TECHNICAL DOCUMENTATION OF LIMITED USE AND INTEREST. THEY ARE PRIMARILY WORKING PAPERS INTENDED FOR INTERNAL USE. THEY CARRY AN IDENTIFYING NUMBER WHICH INDICATES THEIR TYPE AND THE NUMERICAL CODE OF THE ORIGINATING DEPARTMENT. ANY DISTRIBUTION OUTSIDE DTNSRDC MUST BE APPROVED BY THE HEAD OF THE ORIGINATING DEPARTMENT ON A CASE-BY-CASE BASIS.